Available online at www.sciencedirect.com

ScienceDirect

Virology 363 (2007) 288–302

VIROLOGY

www.elsevier.com/locate/yviro

Heterologous viral RNA export elements improve expression of severe acute respiratory syndrome (SARS) coronavirus spike protein and protective efficacy of DNA vaccines against SARS

Benoît Callendret [a], Valérie Lorin [a], Pierre Charneau [b], Philippe Marianneau [d], Hugues Contamin [d,1], Jean-Michel Betton [c], Sylvie van der Werf [a], Nicolas Escriou [a,*]

[a] *Unité de Génétique Moléculaire des Virus Respiratoires, URA CNRS 1966, EA 302 Université Paris 7, France*

[b] *Groupe à 5 ans de Virologie Moléculaire et de Vectorologie, France*

[c] *Unité de Biochimie Structurale, URA CNRS 2185, Institut Pasteur, 25 rue du Dr. Roux, 75724 PARIS Cedex 15, France*

[d] *Unité de Biologie des Infections Virales Emergentes, Institut Pasteur, IFR 128 BioSciences Lyon-Gerland, 21 avenue Tony Garnier, 69365 Lyon Cedex 07, France*

Received 10 October 2006; returned to author for revision 19 December 2006; accepted 15 January 2007

Available online 28 February 2007

Abstract

The SARS-CoV spike glycoprotein (S) is the main target of the protective immune response in humans and animal models of SARS. Here, we demonstrated that efficient expression of S from the wild-type spike gene in cultured cells required the use of improved plasmid vectors containing donor and acceptor splice sites, as well as heterologous viral RNA export elements, such as the CTE of Mazon-Pfizer monkey virus or the PRE of Woodchuck hepatitis virus (WPRE). The presence of both splice sites and WPRE markedly improved the immunogenicity of S-based DNA vaccines against SARS. Upon immunization of mice with low doses (2 μg) of naked DNA, only intron and WPRE-containing vectors could induce neutralizing anti-S antibodies and provide protection against challenge with SARS-CoV. Our observations are likely to be useful for the construction of plasmid and viral vectors designed for optimal expression of intronless genes derived from cytoplasmic RNA viruses.

Keywords: Coronavirus; Severe acute respiratory syndrome; Spike glycoprotein; Viral RNA export element; CTE; WPRE; DNA vaccine

Introduction

A severe, contagious and atypic pneumopathy, named severe acute respiratory syndrome (SARS), emerged in Southern China in late 2002. The etiological agent was found to be a new coronavirus (SARS-CoV). Between November 2002 and July 2003, the virus spread to 29 different countries and was responsible for 8096 clinical cases, leading to 774 deaths (WHO, 21 April 2004, posting date).

The mechanisms of SARS-CoV introduction into humans are largely unknown. SARS-CoV-like viruses have been isolated from caged Himalayan palm civets and raccoon dogs in live-animal markets in China (Guan et al., 2003; Kan et al., 2005). Evidences for direct transmission of SARS-CoV-like viruses from these animals to humans have been reported (Song et al., 2005; The Chinese SARS Molecular Epidemiology Consortium, 2004). However, recent studies suggested that civets may have served only as an amplification host for SARS-CoV and the existence of an upstream wild animal reservoir has been proposed (Tu et al., 2004; Wu et al., 2005). Consistent with this hypothesis, SARS-CoV like viruses sharing more than 88% nucleotide identities with SARS-CoV have been isolated from horseshoe bats in mainland China (Li et al., 2005) and Hong

* Corresponding author. Unité de Génétique Moléculaire des Virus Respiratoires, URA CNRS 1966, Institut Pasteur, 25 rue du Dr. Roux, 75724 Paris Cedex 15, France. Fax: +33 140613241.

E-mail addresses: benoitcl@pasteur.fr (B. Callendret), vlorin@pasteur.fr (V. Lorin), charneau@pasteur.fr (P. Charneau), marianneau@cervi-lyon.inserm.fr (P. Marianneau), Hugues.Contamin@mdsinc.com (H. Contamin), jmbetton@pasteur.fr (J.-M. Betton), svdwerf@pasteur.fr (S. van der Werf), escriou@pasteur.fr (N. Escriou).

[1] Present address: MDS Pharma Service, les Oncins, 69210 Saint Germain sur l'Arbresle, France.

0042-6822/$ - see front matter © 2007 Elsevier Inc. All rights reserved.
doi:10.1016/j.virol.2007.01.012

Kong SAR (Lau et al., 2005). Thus, re-emergence of SARS-CoV is a matter of concern and an efficient vaccine would be the most effective way to control a new epidemic.

Similar to other coronaviruses, SARS-CoV is an enveloped positive-strand RNA virus. Its large single-stranded genome, 29.7 kb in length, encodes the replicase polyproteins, small accessory proteins and four major structural proteins: the nucleoprotein (N), the small envelope protein (E), the membrane protein (M), and a large, club-shaped spike protein (S). The SARS-CoV spike protein is a type-I transmembrane glycoprotein consisting of 1255 amino acids (a.a.), with a molecular weight of ~180 kDa. As predicted by sequence analysis, it consists of four domains: a signal sequence (a.a. 1 to 14), a large ectodomain comprised of amino-acids 15 to 1190 with 23 potential *N*-glycosylation sites, a transmembrane domain (a.a. 1191 to 1227), and a short cytoplasmic tail of 28 a.a. (Ksiazek et al., 2003; Rota et al., 2003). The S protein mediates many of the biological properties of the virus, including viral entry: binding to cellular receptors, ACE2 (Li et al., 2003) and L-SIGN (Jeffers et al., 2004), penetration and fusion between the viral and cellular membranes (Matsuyama et al., 2005; Petit et al., 2005; Simmons et al., 2005). It is also associated with host range and tissue tropism (Giroglou et al., 2004; Qu et al., 2005), as for other coronaviruses (Casais et al., 2003; Haijema et al., 2003; Kuo et al., 2000).

The S protein of SARS-CoV is a candidate antigen for vaccine development, as it is the main target for neutralizing antibodies in human patients (He et al., 2005; Nie et al., 2004; Temperton, 2005; Traggiai et al., 2004). Moreover, passive immunization studies demonstrated that spike-specific neutralizing antibodies are protective in the mouse (Subbarao et al., 2004) and ferret (ter Meulen et al., 2004) animal models. Accordingly, several candidate vaccines relying on the induction of spike-specific neutralizing antibodies have been reported to induce a protective immune response in various animal models (Bisht et al., 2004, 2005; Buchholz et al., 2004; Bukreyev et al., 2004; Chen et al., 2005; Yang et al., 2004).

Efficient expression of intronless genes from plasmid or viral vectors may require the presence of additional cis-acting regulatory modules within the expression cassettes, such as splice sites (SS), retroviral constitutive transport elements (CTE) and hepadnaviral posttranscriptional regulatory elements (PRE). The most studied of these latter viral elements are the CTE of Mason-Pfizer Monkey virus (MPMV-CTE) (Rizvi et al., 1996) and the PRE of Woodchuck Hepatitis virus (WPRE) (Donello et al., 1998) and both have been successfully used for that purpose (Loeb et al., 1999; Tan et al., 1995; Wodrich et al., 2000; Zufferey et al., 1999). However, the optimal choice of posttranscriptional enhancer modules depends on the type of cDNA to be expressed (Schambach et al., 2000). Whether this strategy may apply to the expression of genes from cytoplasm-replicating RNA viruses, which mRNAs are not naturally processed by splicing and nuclear-export machineries, remains to be determined.

In the present study, we report the construction of a series of DNA expression vectors containing the wild-type S coding sequence. The influence of SS, MPMV-CTE or WPRE on expression of S protein in transfected cells and on induction of a protective SARS-CoV-specific immunity in mice after naked DNA immunization are compared. We found that WPRE together with SS allowed most efficient expression of S in 293T and VeroE6 cells whereas CTE had a slight to moderate effect depending on the cell line. Furthermore, dose range experiments demonstrated that, when administered to mice, DNA plasmid vectors with WPRE induced the highest levels of anti-S antibodies and protection towards a challenge with live SARS-CoV.

Results

Construction of SARS-CoV S expression vectors and comparison of S expression in transfected primate cells

The coding region of SARS-CoV S protein was amplified by RT-PCR from the broncho-alveolar lavage of a patient hospitalized with probable SARS at the Hanoï French Hospital (Vietnam) in 2003 and cloned into pcDNA3.1 and pCI expression vectors under the control of the cytomegalovirus (CMV) immediate/early promoter, yielding pcDNA-S and pCI-S plasmids, respectively (see Fig. 2A).

We initially tested protein expression driven by these vectors in transiently transfected Vero E6 cells, which are permissive for SARS-CoV replication, thus allowing mature expression of essential SARS-CoV genes. pcDNA-S did not induce detectable levels of S protein either by immunoblotting using an S-specific rabbit antiserum (Fig. 1, lane 2) or by indirect immunofluorescence (data not shown). This was not due to inadequate sensitivity of the detection methods, since S as

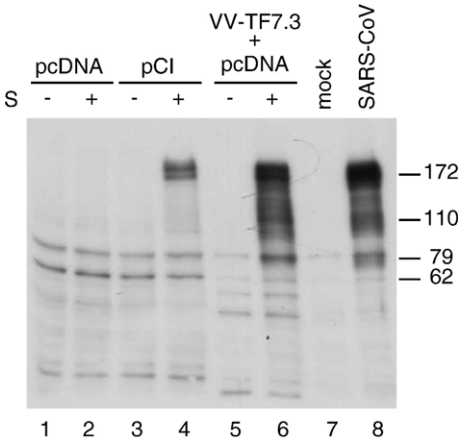

Fig. 1. Transient expression of the SARS-CoV spike protein following plasmid DNA transfection. Subconfluent monolayers of Vero E6 cells were transfected with empty (−) or S (+) expression plasmids. At 48 h post-transfection, whole cell extracts were prepared in Laemmli sample buffer, separated by SDS-PAGE as indicated (lanes 1 to 4) and analyzed by Western blot as described in Materials and methods using rabbit polyclonal antibodies directed against the S protein. Alternatively, VeroE6 cells were infected with VVTF7-3 at a MOI of 5, transfected 1 h later with the indicated construct and analyzed for S expression 18 h thereafter (lanes 5 and 6). As controls, whole cell extracts prepared from VeroE6 cells either mock infected (lane 7) or infected with SARS-CoV (lane 8) were analyzed. The position of the molecular weight markers is shown on the right of the gel (kDa).

expressed in SARS-CoV infected cells was readily detected at the expected size of ~180 kDa (Fig. 1, lane 8). In addition, potential defect in the pcDNA-S construct, low transfection efficiency or other flaws could be excluded, since pcDNA-S induced high levels of S expression from the T7 RNA polymerase promoter, when T7 RNA polymerase was expressed in Vero E6 cells after superinfection with VV-TF7.3 recombinant vaccinia virus (Fig. 1, lane 6).

In contrast, S protein expression could be detected in Vero E6 cells after transfection of the pCI-S construct (Fig. 1, lane 4). Similar data were obtained in 293T cells (see Fig. 2B). The pCI-S construct differs markedly from the pcDNA-S construct by the presence of a chimeric intron between the CMV promoter and the S coding sequence. The inserted intron is composed of the donor site from the first intron of the human β-globin gene and the branch and acceptor site from the intron of an immunoglobulin gene (Promega, January 2004, revision date). These results suggested that the presence of an intron is required for expression of the SARS-CoV S gene, when the corresponding mRNA is synthesized in the nucleus of transfected cells. However, expression levels driven by pCI-S remained low as compared to the levels observed in the T7 RNA polymerase based expression system (Fig. 1, compare lanes 4 and 6). In the latter (Fuerst et al., 1986), transcription takes place primarily in the cytoplasm, suggesting that S mRNA might be abnormally processed after synthesis in the nucleus or inefficiently exported to the cytoplasm.

Enhancement of SARS-CoV S protein expression with viral export elements

Cis-acting viral export elements such as the CTE of Mason-Pfizer Monkey Virus (MPMV-CTE), and the PRE of Woodchuck hepatitis virus (WPRE) have been shown to increase the nuclear export of mRNAs, resulting in higher protein expression levels (Bray et al., 1994; Donello et al., 1998; Gruter et al., 1998; Popa et al., 2002). Therefore, MPMV-CTE and WPRE sequences were inserted in both pcDNA-S and pCI-S plasmids downstream of the S coding sequence and upstream of the polyadenylation sequence (Fig. 2A).

Immunoblot analysis of cell lysates prepared from transfected VeroE6 and 293T cells are shown in Figs. 2B and C, respectively. S expression remained below detectable levels whatever viral export element inserted in the pcDNA-S plasmid. In marked contrast, both CTE and WPRE increased S expression when inserted in the pCI-S plasmid. The most dramatic effect was observed upon pCI-S-WPRE transfection into either VeroE6 or 293T cells. Similar data were obtained in simian FRhK-4 and hamster BHK cells (data not shown). To evaluate more accurately the impact of CTE and WPRE on S production, protein expression levels were quantified from the luminescence signals recorded with a cooled CCD camera (Table 1). As compared to pCI-S, a 12- to 42-fold increase for the WPRE-containing pCI plasmid was observed, regardless of the cell lines used, while CTE had more impact on S expression in VeroE6 cells (9- to 26-fold increase) than in 293T cells (4-fold increase).

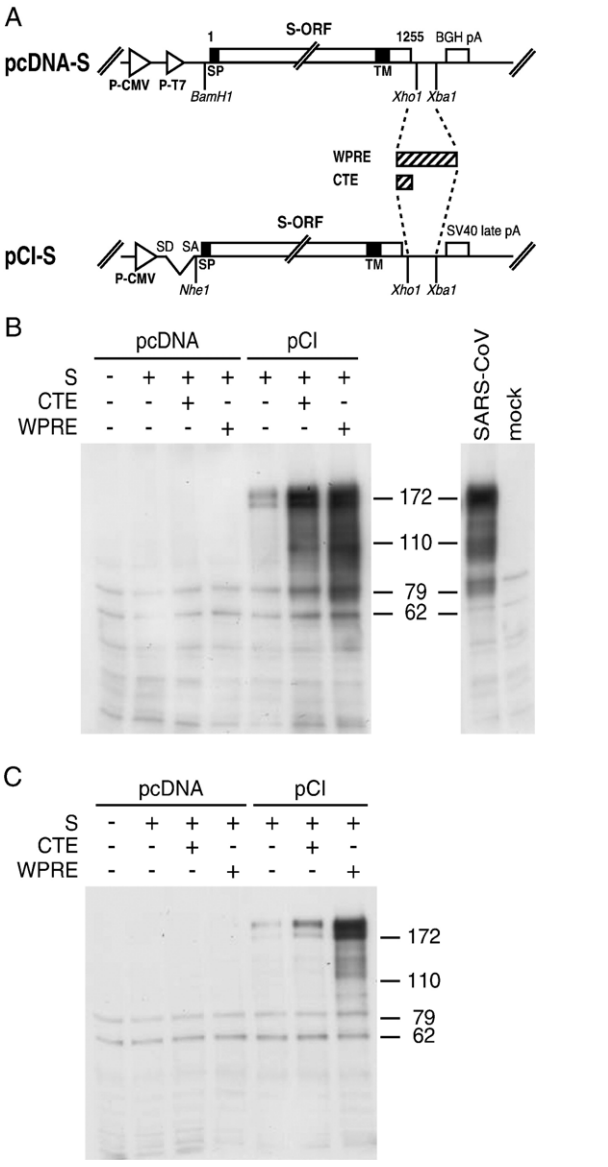

Fig. 2. Improvement of SARS-CoV spike protein expression by viral export elements. (A) Schematic representation of S expression plasmids. Viral export elements were inserted in pcDNA-S and pCI-S plasmids, downstream of the S ORF sequence and upstream of the polyadenylation signal (pA). SP: signal peptide. TM: transmembrane domain. SD-SA: donor and acceptor splice sites, respectively. BGH: bovine growth hormone. SV40: Simian Virus 40. WPRE: Woodchuck hepatitis virus post-transcriptional element. CTE: constitutive transport element from Mason Pfizer Monkey Virus. Subconfluent monolayers of VeroE6 (B) and 293T (C) cells were transfected with the indicated S expression constructs. At 48 h post-transfection, whole cell extracts were analyzed by Western blotting as in Fig. 1. The position of the molecular weight markers is shown on the right of the gel (kDa).

Expression of S at the cell surface was examined by FACS analysis performed on non-permeabilized 293T cells at 48 h post-transfection. Less than 5% of cells transfected with either plasmid from the pcDNA-S series were stained by polyclonal mouse anti-S antibodies (Fig. 3, upper left panel and data not shown), while 50% of cells transfected with the pCI-S-WPRE construct were found positive (Fig. 3, lower right panel). In agreement with immunoblotting data, WPRE was much more

Table 1
Relative quantitative expression of S protein in transiently transfected cells

Plasmid	S levels (arbitrary units)[a]			
	VeroE6 cells[b]		293T cells[b]	
	Expt. 1[c]	Expt. 2	Expt. 1	Expt. 2
pCI	NA	NA	NA	NA
pCI-S	1.0±0.1	1.0	1.0	1.0
pCI-S-CTE	9.8±0.9	26.4	4.6	4.0
pCI-S-WPRE	20.1±2.0	42.3	27.6	12.8

NA: not applicable.
[a] Protein expression levels were quantified from the captured gel image as described in Materials and methods and are indicated in arbitrary units (1=the value measured in pCI-S-transfected cells for a given cell line).
[b] Data from two independent experiments are reported.
[c] Figures are mean±S.D. of duplicate determinations.

efficient than CTE in enhancing S expression from pCI-S DNAs at the surface of 293T cells. Levels of S produced upon transfection of pCI-S-CTE and pCI-S-WPRE were 2- and 11-fold higher, respectively, than those produced upon transfection of pCI-S.

To analyze whether enhanced S expression correlated with increased S mRNA levels, we performed Northern blot analysis of cytoplasmic fractions prepared 24 or 48 h post-transfection of VeroE6 and 293T cells. S mRNAs were detected with a mixture of three S-specific probes and their relative abundance was calculated using β-actin mRNA levels as an internal control. A representative experiment is shown in Fig. 4 for mRNAs prepared 48 h after transfection of 293T cells. No S-specific mRNA was detected in the cytoplasm of cells transfected with any pcDNA-S-derived plasmid or empty plasmid, in agreement with the lack of S expression. S mRNAs of the expected size were observed with plasmids of the pCI-S series. Thus, cytoplasmic accumulation of S mRNA and hence S protein expression appeared to be dependent on correct splicing. Surprisingly, CTE had no impact on the amount of cytoplasmic S mRNAs in VeroE6 and 293T cells, neither at 24 h nor at 48 h post-transfection (Fig. 4 and data not shown). In contrast, WPRE increased mRNA levels in 293T cells by 3-fold at both 24 h (data not shown) and 48 h (Fig. 4) post-transfection, and transiently increased mRNA levels in VeroE6 cells at 24 h post-transfection (2.7 fold increase; data not shown).

Altogether, our results showed that both CTE and WPRE have a greater effect at the protein level than at the mRNA level (compare Fig. 3 and Table 1 to Fig. 4) and thus promote SARS-CoV spike protein expression by increasing mRNA translation. In all cell lines examined, the impact of WPRE on S protein expression was consistently better than that of CTE, reflecting synergistic effects of this element on cytoplasmic mRNA levels and mRNA translation.

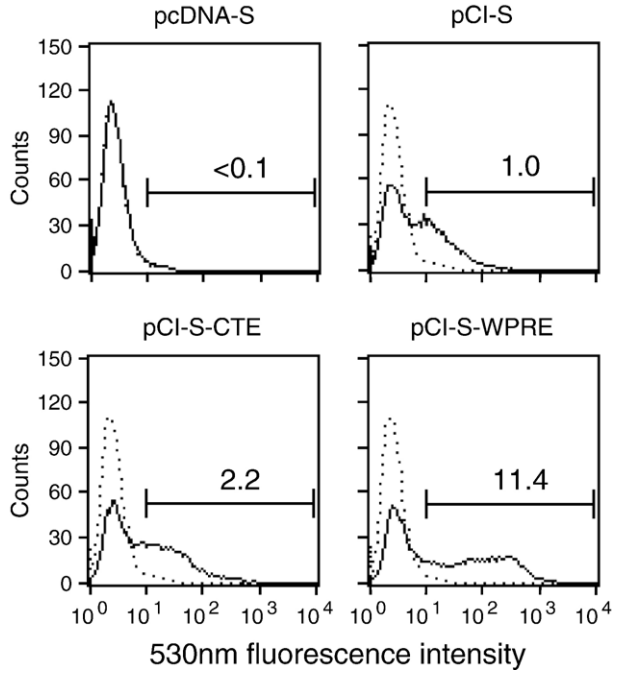

Fig. 3. Analysis of S protein expression at the surface of transfected cells. Subconfluent monolayers of 293T cells were transfected with each of the indicated S expression plasmids. At 48 h post-transfection, cells were detached from the plates and labeled with anti-S mouse polyclonal antibodies and FITC-conjugated anti-mouse IgG antibodies. Flow cytometry analysis was performed on a FACScalibur fluorocytometer. pCI-transfected 293T cells were used as control (dotted lines). S expression at the cell surface of transfected cells was quantified as the mean fluorescence intensity of the fraction of S-expressing cells (bar) and is indicated in each histogram in arbitrary units (1=mean intensity measured in pCI-S-transfected cells).

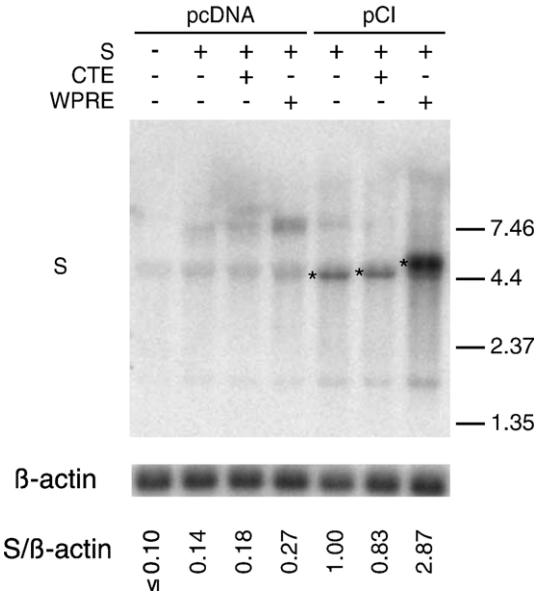

Fig. 4. Analysis of S mRNA in transfected cells. Subconfluent monolayers of 293T cells were transfected with each of the indicated S expression plasmids. At 48 h post-transfection, cytoplasmic RNA was prepared and analysed by Northern blot for the presence of S mRNAs with a mixture of negative sense riboprobes specific for S sequences, as described in Materials and methods. The position of molecular weight markers is indicated on the side. For normalization, Northern blot analysis was performed in parallel using a negative sense β-actin specific riboprobe. The amounts of S specific RNAs of the expected size (stars) and β-actin RNAs were quantified and the calculated S/β-actin specific mRNA ratios are indicated below the images (1=ratio found in pCI-S transfected cells).

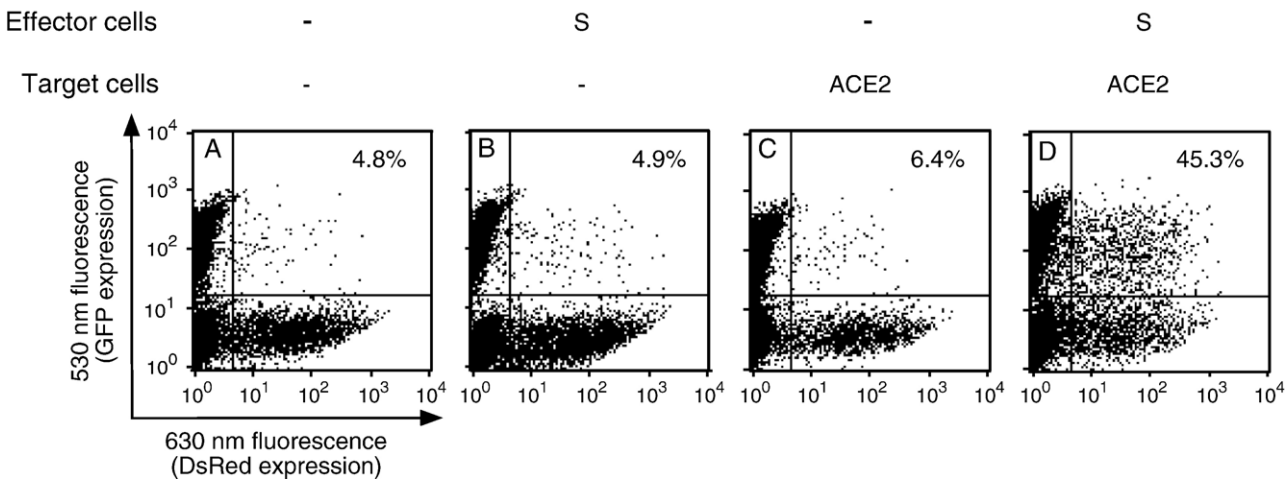

Fig. 5. Efficient fusion of S-protein- and ACE2-expressing 293T cells. 293T cells constitutively expressing GFP (effector cells), were transfected with pCI-S-WPRE or, as control, with the empty pCI plasmid. 293T cells transfected with pCMV-DsRed (target cells) were also transfected with either pcDNA-ACE2 or, as control, with the empty pcDNA plasmid. At 36 h post-transfection, target and effector cells were mixed at a 1:1 ratio and analysed by flow cytometry for GFP and DsRed expression 12 h thereafter. The indicated percentage of fusion was measured as the ratio between double-stained cells (upper right quadrant) and red target cells (lower plus upper right quadrant). A: Effector cells transfected with pCI mixed with target cells transfected with pcDNA. B: Effector cells transfected with pCI-S-WPRE mixed with target cells transfected with pcDNA. C: Effector cells transfected with pCI mixed with target cells transfected with pcDNA-ACE2. D: Effector cells transfected with pCI-S-WPRE mixed with target cells transfected with pcDNA-ACE2.

WPRE-mediated expression of SARS-CoV S allows functional studies of the protein and serological surveillance of SARS

Having shown that the SARS-CoV S protein can be efficiently expressed at the cell surface by using the WPRE element, we sought to further test whether the S protein expressed in this system was functional and antigenically relevant.

We first evaluated the capacity of the WPRE-expressed S protein to induce receptor-dependent cell-to-cell fusion. We took advantage of the fact that, under our experimental conditions, co-transfection of 293T cells with two different expression plasmids allowed expression of both encoded proteins in more than 90% of the transfected cell population (data not shown). Thus, target cells were prepared by co-transfection of 293T cells with pcDNA-DsRed and pcDNA3-ACE2, which allow expression of the fluorescent DsRed protein and the ACE2 SARS-CoV receptor, respectively (Li et al., 2003). Concurrently, effector cells were prepared by transfection of 293T-GFP cells with the pCI-S-WPRE plasmid. The

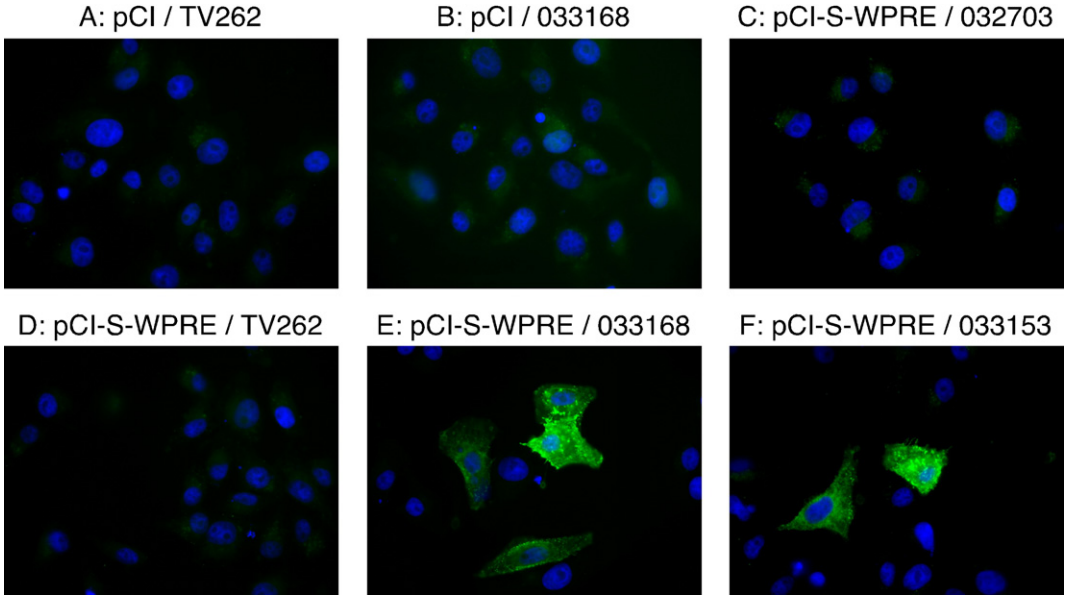

Fig. 6. Serological evaluation of convalescent human sera using S-protein-expressing VeroE6 cells. Subconfluent monolayers of VeroE6 cells were transfected with pCI (A, B) or pCI-S-WPRE (C to F). At 48 h post-transfection, cells were stained as described in Materials and methods using either serum from patient A (#033168; B, E), or serum collected from patient B 8 days (#032703; C) or 29 days (#033153; F) after the onset of SARS symptoms, or serum collected before the SARS epidemic from a healthy donor (TV262; A, D).

fusion of co-cultured green effector cells and red target cells was evaluated by FACS analysis (Fig. 5). We found that no cell-to-cell fusion occurred when S-expressing effector cells were mixed with mock-transfected target cells (panel B) or when mock-transfected effector cells were mixed with ACE2-expressing target cells (panel C), as the percentage of green- and red-stained cells did not increase above background (panel A). In contrast, more than 45% of target cells expressing ACE2 did fuse with effector cells expressing S (panel D).

Next, we evaluated the antigenicity of the WPRE-expressed S protein using convalescent human sera. VeroE6 cells were transfected with pCI-S-WPRE or pCI as a control, and immunofluorescence assays (IFA) were carried out using three SARS convalescent human sera and two normal human sera (Fig. 6). S-expressing VeroE6 cells were readily stained with convalescent sera from the SARS cases (panels E, F and data not shown) but not with sera from healthy blood donors (panel D as an example), while control Vero cells showed no staining (panels A, B). In addition, this S-protein based IFA allowed to monitor seroconversion of patients for SARS, using serum samples taken during the acute and convalescent phases of the disease (panels C and F, respectively as an example).

Altogether, our results indicate that WPRE-mediated expression of S is qualitatively and quantitatively relevant, since the resulting polypeptide is capable of inducing cell-to-cell fusion and is efficiently recognized by convalescent human sera.

Induction of anti-S antibody response in mice immunized with WPRE-enhanced naked DNA vaccine

In order to compare the capacity of CTE and WPRE to enhance the efficacy of naked DNA vaccine, we performed a dose response experiment. Female BALB/c mice were immunized by intramuscular injection of 2, 10 or 50 μg of pCI-S, pCI-S-CTE or pCI-S-WPRE naked plasmid DNA. This dose range extended from suboptimal to optimal doses of typical plasmid DNA vaccine in mice and was selected according to our preliminary experiments (data not shown) and published data (Fu et al., 1999; Ulmer et al., 1994; Wang et al., 2000). As control, a group of mice was injected with 50 μg of DNA from the parental pCI plasmid. Mice were boosted at week 4 with the same dose of DNA and the resulting immune responses were analyzed 3 weeks later. Anti-S serum IgG antibody titers were determined for each individual mice by indirect ELISA using SARS-CoV-infected VeroE6 cell lysates as native antigens (Fig. 7). At the optimal 50-μg dose, each of the three S expression plasmids induced a high anti-S IgG response. The log10 serum IgG titers were 3.7±0.2 for both pCI-S and pCI-S-CTE-immunized mice and 3.9±0.1 for pCI-S-WPRE-immunized mice, indicating that pCI-S-WPRE induced significantly higher (~2-fold, $p<0.05$) anti-S IgG levels than pCI-S and pCI-S-CTE. At the 10-μg suboptimal dose of plasmid DNA, pCI-S-WPRE induced a much higher and more consistent response across mice (3.6±0.2 log10 titer) than pCI-S (2.8±0.4 log10 titer, $p<0.01$) and pCI-S-CTE (2.4±1.0 log10 titer, $p<0.03$). At the lowest dose (2 μg plasmid DNA per mouse), both pCI-S and pCI-S-CTE failed to induce any

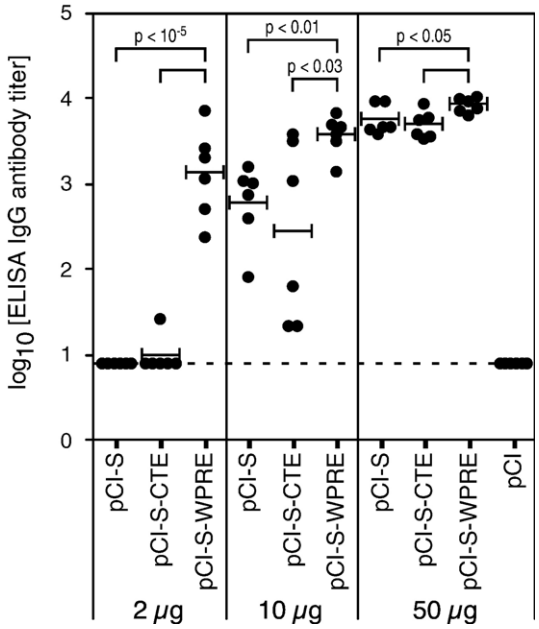

Fig. 7. WPRE enhances anti-S antibody responses in mice immunized with low doses of plasmid DNA. Groups of 6 BALB/c mice were injected twice intramuscularly at 4-week interval with 2, 10 or 50 μg of S expression plasmid DNA as indicated, or with 50 μg of pCI plasmid DNA as control. Immune sera were collected 3 weeks after the second injection. SARS-CoV specific IgG antibody titers were determined by indirect ELISA using SARS-CoV infected VeroE6 cell lysates as the capture antigen, as described in Materials and methods. Values for each individual mouse are represented with black circles, and means with horizontal bars. The detection limit of the assay is indicated by a dotted line.

detectable anti-S antibodies (log10 titer <0.9) with the exception of a single mouse (1.4 log10 titer) out of eight pCI-S-CTE-immunized mice, whereas anti-S IgG titers remained high (3.1±0.5 log10 titer) for all pCI-S-WPRE-immunized mice. Thus, the anti-S antibody levels induced by pCI-S-CTE were comparable to those induced by the pCI-S construct, with no statistically significant differences at any dose tested ($p>0.3$).

This dose response experiment clearly demonstrates that WPRE strongly enhances the immunogenicity of an S-based anti-SARS naked DNA vaccine in mice, whereas CTE has no effect. The most remarkable effect was observed at the very low dose of 2 μg naked DNA per mouse, for which the WPRE-enhanced DNA vaccine only was able to induce high levels of anti-SARS antibodies.

Induction of complete protection of mice against a SARS-CoV challenge by a low dose of WPRE-enhanced DNA vaccine

To assess whether a low dose of the WPRE-enhanced DNA vaccine could induce protective immunity against SARS, BALB/c mice were injected three times with 2 μg of plasmid DNA at 4-week intervals. The mice received the various DNA constructs as described above. First, sera were sampled at 3 weeks post-immunization, and we examined whether the antibody response was capable of SARS-CoV neutralization. Neutralizing antibody titers remained below the detection level

after injection of either pCI-S or pCI-S-CTE plasmid DNA (Fig. 8A). In contrast, significant levels of SARS-CoV neutralizing antibodies were measured in 7 out of 8 mice immunized with pCI-S-WPRE plasmid DNA. Next, at 8 weeks post-immunization, mice were transferred to a BSL-4 animal facility and challenged by intranasal inoculation of 10^5 pfu of SARS-CoV.

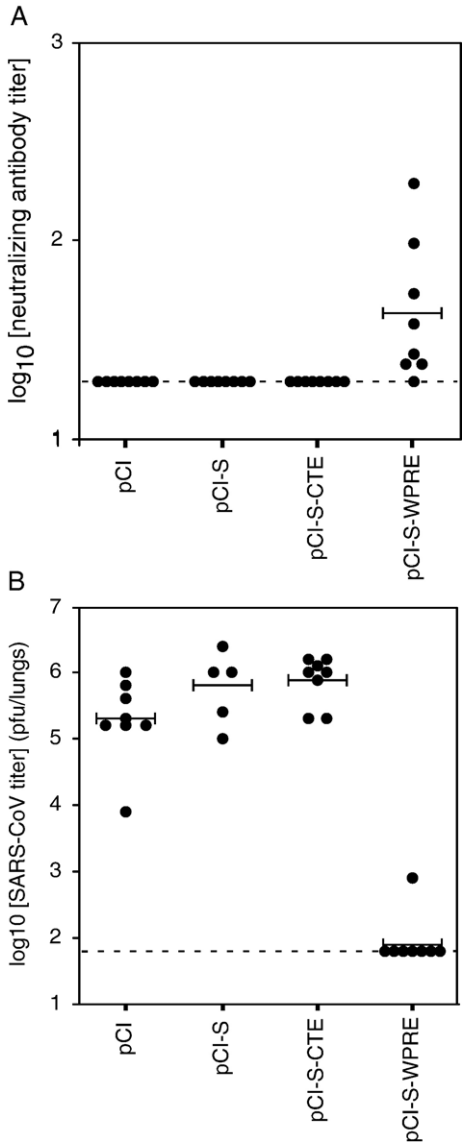

Fig. 8. WPRE is required for protection of mice from SARS-CoV challenge upon immunization with low-dose plasmid DNA. Groups of 8 BALB/c mice were injected three times intramuscularly at 4-week interval with 2 μg of S expression plasmid DNA as indicated, or with 2 μg of pCI plasmid DNA as control. Immune sera were collected 3 weeks after the third injection and assayed for neutralizing antibodies against SARS-CoV. Neutralization titers (A) were calculated as the reciprocal of the highest dilution of each individual serum, which completely prevented SARS-CoV CPE in 50% of the wells, as described in Materials and methods. Eight weeks after the third DNA injection, mice were challenged intranasally with SARS-CoV (10^5 pfu/mouse). Two days after inoculation, mice were euthanized. Lung homogenates were prepared and titrated for infectious SARS-CoV by plaque assay on VeroE6 cells. Viral titers were expressed as $\log_{10}$ (pfu/lungs) for individual mice (B). Values for each individual mouse are represented with black circles, and means with horizontal bars. The detection limits of the assays are indicated by a dotted line. Data shown are from one experiment representative of two.

Viral loads in the lungs were evaluated 2 days later (Fig. 8B). No significant difference was found in the viral titers observed in mice injected with pCI-S (5.8±0.5 log10 pfu/lungs), pCI-S-CTE (5.9±0.3 log10 pfu/lungs) or with control pCI (5.3±0.6 log10 pfu/lungs). In sharp contrast, immunization with pCI-S-WPRE plasmid DNA conferred almost complete protection with no infectious virus detectable in 7 out of 8 mice (log10 pfu/lungs <1.8) and a very low residual titer in a single mouse ($p<10^{-8}$).

These studies clearly indicate that the WPRE-enhanced SARS DNA vaccine is most effective in inducing complete protective immunity, providing protection against SARS-CoV challenge after low-dose injection of naked plasmid DNA.

Discussion

To our knowledge, the vast majority of published studies relying on the transient expression of the spike protein of all coronaviruses before the SARS-CoV epidemic was recognized, involved the use of either T7 RNA polymerase-based expression systems or viral expression vectors such as recombinant Sindbis or vaccinia viruses (Horsburgh and Brown, 1995; Krueger et al., 2001; Narayanan et al., 2003; Pulford and Britton, 1991; Vennema et al., 1996; Yoo and Deregt, 2001). This may be indicative of the difficulty to express efficiently the long coronavirus S gene following transient transfection of mammalian cells with conventional DNA expression vectors, that lead to mRNA synthesis in the cell nucleus. Consistent with this hypothesis, we also found that the SARS-CoV S gene is not expressed at detectable levels when cloned into the classical pcDNA mammalian expression vector under the control of a nuclear polymerase II promoter (Fig. 1), whereas it is expressed efficiently from a recombinant vaccinia virus (V. Lorin, B. Callendret, S. van der Werf and N. Escriou, unpublished data). Likewise, it has been reported that the S protein from SARS-CoV is poorly expressed following DNA transfection (Chang et al., 2006; Hofmann et al., 2004; Qin et al., 2004; Simmons et al., 2004), hence most published studies used T7 RNA polymerase-based expression systems (Schwegmann-Wessels et al., 2004; Xiao et al., 2003) or synthetic genes optimized for human codon usage (Huang et al., 2004; Qin et al., 2004; Zhi et al., 2005). Here, we describe the design and use of a modified DNA expression vector to enhance SARS-CoV S expression in mammalian cells. This DNA vector contains the CMV immediate/early promoter, a chimeric intron and a cis-acting CTE or WPRE element. We demonstrate that this vector permits the expression of high levels of S at the cell surface of transiently transfected cells, that are compatible with functional and antigenic characterization of the S protein. In addition, this low-cost and easy-to-use expression vector allowed us to develop a cell-to-cell fusion assay and an immunofluorescence assay, which may prove useful for the study of cellular and viral determinants of S-induced membrane fusion and for the sensitive and specific routine diagnosis of SARS seroconversion.

Detectable expression of both spike mRNA and protein in transfected cells required the use of plasmid vectors containing

an intron upstream of the S ORF (Figs. 1 and 2). Our findings are consistent with data reported by Hofmann et al. (2004), Simmons et al. (2004) and Broer et al. (2006), who employed the pCAGG or phCMV vectors to achieve detectable S expression. Both pCAGG and phCMV vectors also harbor donor and acceptor splice sites downstream of a polymerase II promoter. Altogether, these data indicate that cytoplasmic accumulation of S mRNA, hence S protein expression, are absolutely dependent on splicing. Most genes in higher eucaryotes contain at least one intron and many studies have clearly shown that constitutively spliced introns or the presence of a heterologous intron of either viral or cellular origin may be required for optimal gene expression in a variety of systems, including transient expression in mammalian tissue culture cells. The importance of splicing for expression of a given gene appears to depend on several factors such as intron and exon identity and cell type (Buchman and Berg, 1988; Petitclerc et al., 1995). Albeit much less documented, the expression of intronless genes of bacterial and viral origin can also be enhanced by including introns within mammalian vectors (Huang and Gorman, 1990; Huang and Yen, 1995). Although it has been suggested that introns alter the nucleocytoplasmic distribution of mRNAs, more recent data indicate that splicing rather enhances both mRNA production and translational efficiency (Lu and Cullen, 2003; Nott et al., 2003). Our results extend these observations and indicate that the nuclear expression of naturally intronless genes derived from RNA viruses that replicate in the cell cytoplasm may follow the same requirements (presence of an intron) for efficient mRNA accumulation in the cytoplasm.

Although cis-acting viral export elements could compensate for the lack of an intron in the expression of the human β-globin cDNA from a retroviral vector (Schambach et al., 2000), CTE and WPRE did not permit efficient expression of the SARS-CoV S gene from the pcDNA vector and both S mRNA and protein remained undetectable. However, a remarkable boost in S expression was observed when CTE or WPRE was combined with an intron within the pCI vector (Figs. 2 and 3). Interestingly, we did not observe any effect of CTE at the level of S mRNA production in 293T and VeroE6 cells. This was unexpected because CTE-enhanced expression has been linked to CTE-mediated export of mRNAs, conferring rev-independence to HIV-1 gag expression (Bray et al., 1994; Wodrich et al., 2000) and contributing to overcome inhibitory elements of HPV-16 L1 mRNA (Tan et al., 1995). Our results rather support the hypothesis raised by Schambach et al. (2000), according to which CTE is much more efficient in promoting export of unspliced intron-containing retroviral RNA transcripts (Ernst et al., 1997a; Gruter et al., 1998; Kang and Cullen, 1999), than in facilitating the transport of spliced mRNA. In contrast, WPRE enhanced cytoplasmic S mRNA levels by 3-fold in both 293T and VeroE6 cells. Both CTE and WPRE have an export function, but they differ by the mechanisms involved in that CTE binds to the Tap nuclear mRNA export factor (Gruter et al., 1998), while WPRE recruits the cellular Crm1 RNA export factor (Popa et al., 2002). The observation that Tap is also implicated in the export of cellular spliced mRNAs from the nucleus suggests that CTE RNA and spliced mRNAs share a common nuclear export pathway (Braun et al., 1999). This may explain the absence of synergy between intron and CTE in enhancing the cytoplasmic levels of spliced S mRNA in both 293T and VeroE6 cells (Fig. 4). In contrast, WPRE RNA and spliced mRNAs use different factors for nuclear export and our data indicate that these may act synergistically to enhance the cytoplasmic expression of an intron-containing WPRE RNA (Fig. 4). A similar observation was made by Schambach et al., who reported that elevated expression of the human multidrug resistance gene (MDR1) mRNA in SW480 cells depends on the presence of both an intron and WPRE (Schambach et al., 2000).

The effect of CTE and WPRE was more pronounced on S protein levels than on S cytoplasmic mRNAs levels (compare Fig. 3 and Table 1 to Fig. 4), indicating that, in addition to their initially recognized role in mRNA export, CTE and WPRE also act by promoting efficient mRNA translation. Such a role for CTE in mRNA translation has been recently suggested by the groups of Boris-Lawrie and Hammarskjöld (Coyle et al., 2003; Hull and Boris-Lawrie, 2003; Jin et al., 2003). In contrast, it is not in full agreement with the common view that WPRE exerts its effect on protein expression mainly by enhancing 3′ mRNA processing and nucleocytoplasmic transport (Donello et al., 1998; Loeb et al., 1999; Zufferey et al., 1999). To our knowledge, a single report suggested that WPRE may contribute to enhanced cytoplasmic utilization of an intronless EGFP mRNA in addition to its effect on nuclear RNA processing and RNA export (Schambach et al., 2000). Interestingly, the closely related Hepatitis B virus PRE has also been reported to enhance translation of the RNA harboring this element (Lu and Cullen, 2003).

In conclusion to our *in vitro* studies, we demonstrated that the marked enhancing effect of WPRE on S protein expression from spliced S transcripts is due to the synergistic effect of increased levels of cytoplasmic messenger RNA and increased cytoplasmic utilization of these mRNAs. Our data provide a likely explanation to the observations of Wang et al. (2003) who reported that WPRE improved the production of the E2 protein of the type 2 bovine diarrhea virus (a cytoplasmic RNA virus) when expressed in transiently transfected cells or from a recombinant herpesvirus. Our results have important implications for the construction of plasmid and viral vectors optimally designed for the expression of intronless genes from cytoplasmic RNA viruses.

Successful expression of full-length S protein in mammalian cells was alternatively achieved by others by using codon-optimized synthetic genes (Huang et al., 2004; Qin et al., 2004; Zhi et al., 2005). Codon-usage adaptation most often involves the substitution of nearly every wobble position for a G or C nucleotide (Nakamura, October 2006, posting date; Nakamura et al., 2000), resulting in genes with a much diverse nucleotide composition and decreased A/T content. Wild-type genes from viruses with a nuclear life cycle such as HIV-1 or HPV-16 contain regulatory elements evolved to inhibit mRNA cytoplasmic accumulation. For HIV-1 Gag, Vpu, Vif (Graf et al., 2000; Kotsopoulou et al., 2000; Nguyen et al., 2004) or HPV-16 L1 and L2 proteins (Collier et al., 2002; Oberg et al., 2003),

codon optimization of corresponding genes has been shown to result in the inactivation of such elements, thus leading to increased viral protein expression from nuclear DNA expression vectors. Cytoplasmic viruses, such as SARS-CoV, may contain cryptic splice sites, mRNA instability motifs such as A/U-rich elements (AREs), or putative *cis*-active inhibitory sequences, which may explain why DNA vector-based expression of genes from these viruses is dependent on the presence of heterologous intron and transport elements. It can be hypothesized that codon-usage adaptation is a successful strategy to express high levels of cytoplasmic virus proteins as the result of removal of these yet uncharacterized inhibitory elements.

In S-based DNA vaccination experiments, we found that the presence of an intron was mandatory to induce high titers of protective neutralizing antibodies in immunized mice (data not shown). This is in agreement with the absence of S polypeptide expression in cultured cells from the pcDNA-S plasmid (Figs. 1–3) and with the weak antibody responses observed by others in mice immunized with pcDNA-based S constructs (Wang et al., 2005b). In addition, among published reports describing full-length-S-based DNA vaccines, only those based on a codon-optimized gene proved capable of inducing high titers of neutralizing antibodies in mice (Yang et al., 2004, 2005; Yi et al., 2005) or rabbits (Wang et al., 2005a). It is noteworthy that similar observations were reported recently for replication-defective human adenoviral vectors containing the wild-type S gene under the control of the CMV promoter; such recombinant vectors failed to induce cellular immune responses against spike epitopes, whereas vectors encoding codon-optimized S protein proved to be potent immunogens (Zhi et al., 2005). Since expression from adenoviral vectors relies on nuclear transcription of the foreign gene, this corroborates our hypothesis that wild-type S mRNA does not accumulate in the cytoplasm in the absence of a heterologous intron.

In the present study, we demonstrated that a combination of an intron and WPRE, but not of an intron and CTE, acted synergistically in enhancing the immunogenicity of an S-based anti-SARS DNA vaccine in BALB/c mice. We showed that 10 μg of pCI-S-WPRE induced a SARS-CoV neutralizing antibody response ($\log_{10}$ titer = 2.2 ± 0.2) similar to that induced by 25 μg of a codon-optimized expression vector, as described by Yang et al. (2004). Moreover, our *in vivo* data clearly indicate that immunization with the WPRE-enhanced vaccine induced complete protective immunity against challenge infection with SARS-CoV at doses as low as 2 μg at which the more conventional DNA vaccine (including intron sequence but lacking WPRE) did not (Fig. 8). To our knowledge, this is the first report of a successful DNA vaccination protocol using the full-length, wild-type S gene of SARS-CoV, without codon optimization. Whether WPRE could further enhance the protective efficacy of a DNA vaccine based on a codon-optimized gene of the SARS-CoV S protein, such as that reported by Yang et al., is an interesting question which would deserve additional studies.

It has been reported recently that the presence of WPRE also markedly enhanced the efficacy of two other DNA vaccines, a viral vaccine based on HA expression in a mouse model of influenza (Garg et al., 2004), as well as a tumor vaccine in a mouse model of neuroblastoma metastases (Pertl et al., 2003). The three studies with the SARS (our study), influenza (Garg et al., 2004) and neuroblastoma (Pertl et al., 2003) models show remarkable complementarity in demonstrating that WPRE enhanced the protective efficacy of DNA vaccines encoding antigens from the fully-spliced cDNA of a tumor gene and two naturally intronless genes, one derived from a nucleus-replicating negative strand RNA virus (influenza virus) and the other from a cytoplasm-replicating positive strand RNA virus (SARS-CoV). The mechanisms involved in the enhanced induction of protective immunity remain *stricto sensu* to be investigated but WPRE very likely improves the level of antigen expression *in vivo*, as it does *in vitro* in transient transfection experiments.

In summary, our data provide valuable information with respect to the improvement of S protein expression from the wild-type SARS-CoV gene by using both an intron and the WPRE post-transcriptional enhancer, and resulting improvement of the immunogenicity of an S-based DNA vaccine. From a practical point of view, this may help decrease the amount of plasmid DNA in immunization protocols. As noted by others (Garg et al., 2004), by lowering the amount of DNA used in immunization protocols, concerns raised by the use of DNA vaccines, such as risks posed by integration events into the host genome or the induction of autoimmune responses (Cui, 2005), are minimized. Moreover, one of the principal limitations to DNA vaccine efficacy in large animals, like non-human primates, may be related to the limited distribution of DNA within the injected tissue and limited uptake to the nucleus following injection of DNA vaccine in a relatively small volume (Dupuis et al., 2000; Otten et al., 2004). These limitations may be circumvented by the use of efficient DNA vectors based on a combination of intron and WPRE enhancer, such as those we describe here. Thus, these improved plasmid vectors might possibly contribute to the development of a safe and efficient DNA vaccine against SARS in humans. Further studies in larger animals, such as cynomolgus macaques or African Green Monkeys, which were recently described as suitable animal models for SARS (Fouchier et al., 2003; Lawler et al., 2006; McAuliffe et al., 2004; Rowe et al., 2004) could help validate the intron and WPRE based vectors.

Materials and methods

Cell lines and viruses

FRhK-4 (Fetal Rhesus monkey Kidney), CV-1 and Vero E6 (African Green monkey kidney) cells were grown at 37 °C under 5% CO_2 in complete DMEM [Dulbecco's modified Eagle medium with 4.5 mg/mL L-glucose, 100 U/mL penicillin and 100 μg/mL streptomycin], supplemented with 5% heat-inactivated fetal calf serum (FCS) (DMEM-5). 293T (human kidney) cells were grown in complete DMEM supplemented with 10% FCS (DMEM-10).

SARS-CoV FFM-1 strain (Drosten et al., 2003), was kindly provided by H.W. Doerr (Institute of Medical Virology, Frankfurt University Medical School, Germany). Viral stocks were produced at 35 °C by passage on Vero E6 cell cultures at a multiplicity of infection (M.O.I.) of 0.01 in complete DMEM with 2% FCS. All viral stocks were stored at −80 °C and titrated in a standard limiting dilution assay on Vero E6 cell monolayers in 96-well microtiter plates. Infectious titers were determined as 50% tissue culture infective doses (TCID50) according to Reed and Muench (Reed and Muench, 1938). All work involving infectious SARS-CoV was performed in an enhanced biosafety level 3 containment laboratory with rigorous safety procedures according to WHO guidelines.

VV-TF7.3 is a recombinant vaccinia virus encoding the T7 RNA polymerase (Fuerst et al., 1986) and was provided by B. Moss (National Institute of Health, Bethesda, U.S.A.). VV-TF7.3 was propagated at 35 °C by passage on CV-1 monolayers at an MOI of 0.1 and titrated by a standard plaque assay.

S gene expression plasmids

The S gene of SARS-CoV was obtained directly from the viral RNA extracted with the QIAamp Viral RNA mini kit (Qiagen) from the broncho-alveolar lavage (#031589 specimen) of a patient hospitalized with a diagnosis of probable SARS at the Hanoï French Hospital, Vietnam. Briefly, after reverse transcription of the RNA, overlapping S cDNA fragments were produced by nested PCR and the cDNA fragment representing the complete S gene sequence (nt 21406–25348) was assembled from clones harboring the consensus protein sequence as deduced by direct sequencing of the amplicons from specimen #031589 (Nal et al., 2005). The resulting plasmid pSARS-S was used as the source of S cDNA for subsequent cloning into mammalian expression vectors. Comparison of its sequence with the S sequences of the TOR2 (GenBank accession no. AY274119.3) and Urbani (GenBank accession no. AY278741.1) isolates revealed one amino-acid difference at position 577: Alanine for TOR2 and Serine for Urbani and 031589. The DNA sequence coding for the S protein was amplified by PCR with the PWO polymerase (Roche) using pSARS-S plasmid as a template and oligonucleotides 5′-ATAGGATCCA CCATGTTTAT TTTCTTATTA TTTCTTACTC TCACT-3′ and 5′-ATACTCGAGT TATGTGTAAT GTAATTTGAC ACCCTTG-3′ containing *Bam*HI and *Xho*I restrictions sites. After digestion with *Bam*HI and *Xho*I, the resulting DNA fragment was inserted at the corresponding sites of the pcDNA3.1(+) vector (Invitrogen), yielding plasmid pcDNA-S. Next, the S insert was subcloned between the *Nhe*I and *Xho*I sites of the pCI plasmid (Promega), yielding plasmid pCI-S.

Plasmids containing the constitutive transport element of Mazon-Pfizer Monkey Virus (CTE) (Ernst et al., 1997b) or the post-regulatory element of the Woodchuck Hepatitis Virus (WPRE) (Donello et al., 1998) were kindly provided by Y. Jacob and P. Charneau respectively (Institut Pasteur, Paris, France). The CTE fragment was obtained by digestion of the relevant plasmid with *Xho*I and *Bam*HI. The WPRE fragment was obtained by digestion of the relevant plasmid with *Xho*I and *Kpn*I. These fragments were then inserted downstream the S ORF sequence between the *Xho*I and *Xba*I sites either in pcDNA-S or in pCI-S plasmids, yielding plasmids pcDNA-S-CTE, pcDNA-S-WPRE, pCI-S-CTE and pCI-S-WPRE respectively.

All constructs' inserts were verified by the sequencing of positive clones using a Big Dye terminator sequencing kit and an automated sequencer (Applied Biosystems).

Antibodies

Rabbit anti-S polyclonal antibodies

The cDNA encoding amino acids 475 to 1193 of the S protein was amplified by PCR using the S plasmid as a template and oligonucleotides 5′-CCCATATGAG TGACCTTGAC CGGTGCACCA C-3′ and 5′-CCCCCGGGTT TAATATATTG CTCATATTTT CCC-3′ containing *Nde*I and *Xma*I restriction sites. After digestion with *Nde*I and *Xma*I, the resulting DNA fragment was inserted at the corresponding sites of the bacterial expression vector pIVEX2.4d (Roche), yielding plasmid pIV2.4S_C. The final recombinant fragment of S (S_C) contained an extraneous N-terminal polyhistidine tag. The construct's insert was confirmed by DNA sequencing using a Big Dye terminator sequencing kit and an automated sequencer (Applied Biosystems). Exponentially growing cultures of *Escherichia coli* BL21(DE3)pDIA17 cells harboring the pIV2.4S_C expression construct were induced to synthesize the S_C polypeptide by addition of 1 mM isopropyl-β-D-thiogalactoside. Cells were allowed to grow for 2 h at 30 °C. Under these conditions, the S_C recombinant polypeptide was recovered as inclusion bodies: cells were harvested and lysed in lysis buffer (0.1 M Tris–HCl pH 7.5, 1 mM EDTA) using a French press at 1200 psi. Inclusion bodies in the cell lysate were pelleted by centrifugation at 20,000×*g* for 15 min and washed in lysis buffer supplemented with 2% Triton X100 and 10 mM β-mercaptoethanol and then in 10 mM Tris–HCl, 7 M urea, pH 7.5 buffer for 30 min under gentle shaking, before final resuspension in 10 mM Tris–HCl, pH 7.5. The S_C protein was obtained at a purity of more than 90% as determined by SDS-PAGE and Coomassie blue staining.

New Zealand White rabbits were immunized by intradermal inoculation with 0.5 mg of recombinant S_C polypeptide emulsified in Incomplete Freund's Adjuvant (Sigma) and boosted twice at 3 to 4-week intervals. This was followed 3 weeks later by another injection of recombinant S_C polypeptide, which had been further purified on a sucrose gradient and washed with 2% Triton X100. Immune sera were collected 5 weeks after the last boost. The antibodies reacted specifically with the S protein expressed in SARS-CoV infected VeroE6 cells.

Mouse anti-S polyclonal antibodies

Anti-S antibodies were also raised in mice against the ectodomain of the S protein, expressed in mammalian cells as a soluble polypeptide (B. Callendret, V. Lorin, P. Charneau, S. van der Werf and N. Escriou, unpublished data).

Collection of sera from SARS-CoV-infected patients

The first serum sample (sample #033168) was collected 38 days after the onset of symptoms from patient A with probable SARS, according to the WHO case definition (WHO, October 2004, posting date). The second set of sera consisted of one pair of samples that was collected from patient B with probable SARS, 8 days (sample #032703) and 29 days (sample #033153) after the onset of symptoms. For both patients A and B, respiratory tract specimens were tested positive for the SARS-L gene by nested RT-PCR (Drosten et al., 2003). As a control, serum samples collected before the 2002 SARS epidemic were obtained from healthy blood donors (#TV262 and #TV263). All serum samples were inactivated by two cycles of heating for 30 min at 56 °C and clarified by centrifugation for 5 min at 15,000×*g*.

IgG antibodies against the SARS-CoV were present in both the #033168 and the #033153 serum samples as assayed by indirect ELISA using crude lysates from SARS-CoV infected cells as the coating antigen (see below), and there was no non specific binding of the #TV262 and #TV263 sera to SARS-CoV antigens.

Analysis of S protein expression in transiently transfected cells

10^6 Vero E6 cells or 1.4×10^6 293T cells in 35 mm Petri dishes under 2 mL of DMEM-5 or DMEM-10 culture medium respectively were transfected with 2 μg of plasmid DNA and 6 μL of Fugene6 reagent (Roche), according to manufacturer's instructions and incubated at 37 °C under 5% CO_2. Medium was replaced 24 h later and S expression analyzed at the indicated time by Western blot, cytofluorometry or immunofluorescence assays.

Alternatively, Vero E6 cells (10^6 in 35 mm Petri dishes) were infected at an MOI of 5 with VV-TF7.3 and transfected 1 h later with 2 μg of either pcDNA-S or pcDNA plasmid DNA as described above. Vero E6 cells grown in 12 cm^2 flasks were infected with SARS-CoV FFM-1 strain at an MOI of 2 and incubated in complete DMEM supplemented with 2% FCS at 35 °C under 5% CO_2. Total cell lysates were prepared 18 h after VV-TF7.3 infection or 24 h after SARS-CoV infection, and S expression was analyzed by Western blot.

Western-blot analysis

For Western blot assays, total cell extracts were harvested 48 h post-transfection in 300 μL of Laemmli sample buffer. Samples were denatured by heating at 95 °C for 10 min and sonicated. Proteins were separated by electrophoresis on 8% SDS-polyacrylamide (prosieve 50, Cambrex) gels, and transferred onto a PVDF membrane (Amersham). The membrane was incubated with PBS–0.1% Tween–5% unfatted milk for 1 h at room temperature prior to immunoblotting with rabbit anti-S polyclonal antibodies. Following incubation with peroxydase conjugated anti-rabbit secondary antibody (NA934V, Amersham) the immunoblot was revealed with enhanced chemiluminescence (ECL+, Amersham), according to the manufacturer's instructions and by autoradiography on Hyperfilm (Amersham).

Alternatively, the luminescence signals were captured with a cooled CCD camera (Fluor-S multimager, Bio-Rad). Protein expression levels were quantified from gel images using the Quantity One software (v 4.2.3, Bio-Rad).

Northern blot analysis

VeroE6 and 293T cells grown in 35-mm dishes were transfected as described above. At 24 or 48 h post-transfection, cell monolayers were washed twice in D-PBS (Invitrogen) and cellular RNAs were prepared. Total cellular RNAs were isolated by Trizol-LS extraction (Invitrogen) according to the manufacturer's recommendations. For cytoplasmic RNA extraction, cells were lysed on ice in 10 mM Tris–HCl pH 8.0, 0.14 M NaCl, 1.5 mM $MgCl_2$, 1 mM DTT, 0.5% NP-40. After 10 min of incubation at 4 °C, samples were centrifugated at 10,000×*g* for 2 min, and the RNAs were purified from the supernatant by phenol/chloroform extraction and isopropanol precipitation. The RNAs were treated with DNAse I using the DNA-free kit (Ambion) according to the manufacturer's recommendations and stored at −80 °C until use.

After denaturation at 70 °C in 50% formamide, 2.2 M formaldehyde, 1× running buffer [40 mM MOPS, 10 mM sodium acetate, 2 mM EDTA, pH 7.0], samples (2 μg) were run on a 1.2% agarose–0.6 M formaldehyde gel, blotted onto a nylon membrane (Hybond N, Amersham), and fixed by UV irradiation. The membranes were hybridized with a mixture of 3 negative sense S-specific ^{32}P-labeled riboprobes corresponding to nt 21492–22830, 22830–24374 and 24374–25256 of the SARS-CoV genome. For normalization, the membranes were hybridized with a β-actin-specific riboprobe. Hybridizations were performed at 65 °C in a 50% formamide, 5× SSC, 5× Denhardt, 0.5% SDS solution. The membranes were washed 3 times in 2× SSC, 0.1% SDS at room temperature and another 3 times in 0.1× SSC, 0.1% SDS at 70 °C. Finally, the membranes were exposed on a STORM 820 phosphorimager (Molecular Dynamics) and analyzed using the Image Quant program (v 1.2, Molecular Dynamics).

Cytofluorometry and indirect immunofluorescence assays

For cytofluorometry assays, subconfluent monolayers of VeroE6 cells and 293T cells were transfected as described above. 48 h post-transfection, cells were washed once in D-PBS and detached with 1 mL of cell dissociation solution (Sigma). Cells were stained with polyclonal mouse anti-S antibody for 45 min at 4 °C and, after washing, incubated with secondary antibody (anti-mouse FITC-conjugated, BD Bioscience Pharmingen) for 45 min at 4 °C. Cells were then washed and fixed with PBS–1% paraformaldehyde. Events were acquired on a FACScalibur fluorocytometer (Beckton Dickinson) and analyzed with the BD CellQuest Pro software (v 5.2, Beckton Dickinson).

For indirect immunofluorescence assays, subconfluent monolayers of VeroE6 cells were transfected as described above. 24 h post transfection, cells were dissociated with 1 mL of cell dissociation solution, plated on 20 mm glass coverslips in a 12 well-plate and incubated in DMEM-5 at 37 °C under 5% CO_2. 24 h later, cells were washed in D-PBS and fixed with PBS–4% paraformaldehyde for 15 min. Coverslips were then

incubated for 45 min with patient serum diluted 1/300 in PBS–2% BSA. After subsequent incubation with a FITC-conjugated anti-human IgG secondary antibody (Jackson Immunoresearch), the samples were mounted on slides with DAPI-containing Vectashield (Vector laboratory) and analyzed under an Axioplan 2 epifluorescence microscope (Zeiss). Pictures were acquired with an Axiocam MRm camera and processed with the Axiovision software (v 4.2, Zeiss).

Cell fusion assay

Plasmid pcDNA3-ACE2 encoding the ACE2 molecule, which is a receptor for SARS-CoV, was obtained from Michael R. Farzan (Li et al., 2003). 293T cells, constitutively expressing green fluorescent protein (293T-GFP) were obtained by transduction of 293T cells with the TRIP-GFP lentiviral vector (Zennou et al., 2000).

293T-GFP effector cells were transfected either with plasmids encoding the S glycoprotein or the pCI plasmid as a control, as described above. In parallel, 293T target cells were co-transfected with 3 μg of DsRed plasmid DNA and 3 μg of either pcDNA or pcDNA-ACE2 plasmid DNA using 10 μL Fugene6 transfection reagent. Medium was replaced 24 h after transfection. Effector and target cells were detached 12 h later with cell dissociation solution, resuspended in fresh DMEM-10 and counted. 6×10^5 per well of each target and effector cells were plated together in a 12 well-plate with 1 mL of DMEM-10 in each well and co-cultured for 12 h at 37 °C under 5% CO_2. The cells were then trypsinized, fixed with PBS–1% paraformaldehyde and analyzed on a FACScalibur fluorocytometer. Fusion was measured as the ratio between double-stained and red target cells using the BD CellQuest Pro software.

Animal studies

Immunization of mice

Female BALB/c mice (CERJ) 7 to 8 weeks of age were housed and handled according to the Pasteur Institute guidelines in compliance with European animal welfare regulations. Mice were injected intramuscularly with 100 μL PBS (50 μL in each *tibialis anterior* muscle) containing plasmid DNA. Mice were injected with either 50 μg of pCI plasmid DNA as a control, or variable amounts (2, 10 or 50 μg) of pCI-S, pCI-S-CTE or pCI-S-WPRE plasmid DNA. Booster injections were administered at 3 or 4-week intervals. DNA used for injection was prepared using the EndoFree Plasmid Mega Kit (Qiagen) and tested for the absence of endotoxin (<5 EU/mg), as measured with the QCL-1000 Endotoxin kit (BioWhittaker). Blood from mice was collected 1 week before immunization and 3 weeks after each injection.

Assays for anti-SARS-CoV antibodies

The induction of SARS-CoV specific antibodies in immunized mice was measured by indirect ELISA and neutralization assay.

For ELISA, microtiter plates were coated with SARS-CoV infected or mock-infected Vero E6 crude cell lysates, which had been prepared in a 50 mM Boric Acid, 120 mM NaCl, 1% Triton X-100 solution at pH 9.0, sonicated in a cup-horn tip, clarified by centrifugation at 15,000×*g* for 10 min and inactivated frozen by gamma irradiation with 50 kGy from a ^{60}Co source. After washing in PBS–0.1% Tween, plates were incubated with three-fold serial dilutions of mouse sera in PBS-Tween–3% dry skimmed milk (w/v) starting at 1:16.7 or 1:50. Bound antibodies were revealed with horseradish peroxidase-conjugated anti-mouse IgG secondary antibody (Amersham) and TMB (3,3′-5,5′-tetramethylbenzidine, KPL). The absorbance was measured at 450 nm (reference wavelength: 620 nm). Readings from wells coated with mock lysates were substracted from wells with SARS-CoV lysates and SARS-CoV specific IgG titers were calculated as the reciprocal of the highest dilution of individual serum, giving an absorbance difference of 0.5.

For neutralization assays, two-fold serial dilutions of heat-inactivated (56 °C, 30 min) serum samples were mixed with 100 TCID50 of SARS-CoV in 100 μL complete DMEM, incubated at 37 °C for 60 min and added to a subconfluent monolayer of FRhK-4 cells in a 96-well microtiter plate. Each dilution of serum as well as positive control (100 TCID50 of SARS-CoV) and negative cell controls were tested in quadruplicate and cytopathic effect (CPE) endpoints were read up to 7 days after inoculation. Neutralizing antibody titers were determined according to the Reed and Muench method (Reed and Muench, 1938) as the reciprocal of the highest dilution of each serum, which suppressed CPE in at least 2 out of 4 wells.

Challenge infection of mice with SARS-CoV

Eight weeks after the third plasmid DNA injection, mice were lightly anaesthetized with Isoflurane (Mundipharma) and inoculated intranasally with 10^5 pfu of SARS-CoV in 40 μL PBS. Mice were euthanized 48 h after challenge infection and whole lungs crushed in 500 μL DMEM supplemented with 2% FCS using glass beads and a MM200 Mixer Mill (Retsch). After clarification by low-speed centrifugation for 5 min, lung homogenates were titrated for infectious virus on VeroE6 cells monolayers in a standard plaque assay. Challenge infection of mice and subsequent analysis were done in the "Jean Merieux" biosafety level 4 containment laboratory. Three mice died before transfer to the BSL-4 facility, thus could not be challenged. Statistical analysis was performed on the log10 of the viral titers measured for individual mice using the Student's independent *t*-test, with the assumptions used for small samples (normal distribution of the variables and same variance for the populations to be compared).

Acknowledgments

We thank Pr. Dr. H.W. Doerr (Institute of Medical Virology, Frankfurt University Medical School, Germany) for providing us with the SARS-CoV FFM-1 strain and Dr. M.R. Farzan (Department of Medicine, Harvard Medical School, Boston, MA) for providing us with plasmid pcDNA3-ACE2. We also thank Drs. Annette Martin and Nadia Naffakh for critical reading of the manuscript and helpful suggestions, Philippe

Loth and Sandra Lacôte for expert technical assistance in performing the SARS-CoV challenge experiment. The assistance of the staff of the WHO Collaborative Center for reference and research on influenza and other respiratory viruses (Institut Pasteur, Paris, France) in initial analysis of the SARS specimens and sera is gratefully acknowledged.

This work was supported in part by grants from GlaxoSmithKline Biologicals and Bio-Rad Laboratories. B.C. was supported by a fellowship from GlaxoSmithKline Biologicals.

References

Bisht, H., Roberts, A., Vogel, L., Bukreyev, A., Collins, P.L., Murphy, B.R., Subbarao, K., Moss, B., 2004. Severe acute respiratory syndrome coronavirus spike protein expressed by attenuated vaccinia virus protectively immunizes mice. Proc. Natl. Acad. Sci. U.S.A. 101, 6641–6646.

Bisht, H., Roberts, A., Vogel, L., Subbarao, K., Moss, B., 2005. Neutralizing antibody and protective immunity to SARS coronavirus infection of mice induced by a soluble recombinant polypeptide containing an N-terminal segment of the spike glycoprotein. Virology 334, 160–165.

Braun, I.C., Rohrbach, E., Schmitt, C., Izaurralde, E., 1999. TAP binds to the constitutive transport element (CTE) through a novel RNA-binding motif that is sufficient to promote CTE-dependent RNA export from the nucleus. EMBO J. 18, 1953–1965.

Bray, M., Prasad, S., Dubay, J.W., Hunter, E., Jeang, K.T., Rekosh, D., Hammarskjold, M.L., 1994. A small element from the Mason-Pfizer monkey virus genome makes human immunodeficiency virus type 1 expression and replication Rev-independent. Proc. Natl. Acad. Sci. U.S.A. 91, 1256–1260.

Broer, R., Boson, B., Spaan, W., Cosset, F.L., Corver, J., 2006. Important role for the transmembrane domain of severe acute respiratory syndrome coronavirus spike protein during entry. J. Virol. 80, 1302–1310.

Buchholz, U.J., Bukreyev, A., Yang, L., Lamirande, E.W., Murphy, B.R., Subbarao, K., Collins, P.L., 2004. Contributions of the structural proteins of severe acute respiratory syndrome coronavirus to protective immunity. Proc. Natl. Acad. Sci. U.S.A. 101, 9804–9809.

Buchman, A.R., Berg, P., 1988. Comparison of intron-dependent and intron-independent gene expression. Mol. Cell. Biol. 8, 4395–4405.

Bukreyev, A., Lamirande, E.W., Buchholz, U.J., Vogel, L.N., Elkins, W.R., St Claire, M., Murphy, B.R., Subbarao, K., Collins, P.L., 2004. Mucosal immunisation of African green monkeys (*Cercopithecus aethiops*) with an attenuated parainfluenza virus expressing the SARS coronavirus spike protein for the prevention of SARS. Lancet 363, 2122–2127.

Casais, R., Dove, B., Cavanagh, D., Britton, P., 2003. Recombinant avian infectious bronchitis virus expressing a heterologous spike gene demonstrates that the spike protein is a determinant of cell tropism. J. Virol. 77, 9084–9089.

Chang, C.Y., Hong, W.W., Chong, P., Wu, S.C., 2006. Influence of intron and exon splicing enhancers on mammalian cell expression of a truncated spike protein of SARS-CoV and its implication for subunit vaccine development. Vaccine 24, 1132–1141.

Chen, Z., Zhang, L., Qin, C., Ba, L., Yi, C.E., Zhang, F., Wei, Q., He, T., Yu, W., Yu, J., Gao, H., Tu, X., Gettie, A., Farzan, M., Yuen, K.Y., Ho, D.D., 2005. Recombinant modified vaccinia virus ankara expressing the spike glycoprotein of severe acute respiratory syndrome coronavirus induces protective neutralizing antibodies primarily targeting the receptor binding region. J. Virol. 79, 2678–2688.

Collier, B., Oberg, D., Zhao, X., Schwartz, S., 2002. Specific inactivation of inhibitory sequences in the 5′ end of the human papillomavirus type 16 L1 open reading frame results in production of high levels of L1 protein in human epithelial cells. J. Virol. 76, 2739–2752.

Coyle, J.H., Guzik, B.W., Bor, Y.C., Jin, L., Eisner-Smerage, L., Taylor, S.J., Rekosh, D., Hammarskjold, M.L., 2003. Sam68 enhances the cytoplasmic utilization of intron-containing RNA and is functionally regulated by the nuclear kinase Sik/BRK. Mol. Cell. Biol. 23, 92–103.

Cui, Z., 2005. DNA vaccine. Adv. Genet. 54, 257–289.

Donello, J.E., Loeb, J.E., Hope, T.J., 1998. Woodchuck hepatitis virus contains a tripartite posttranscriptional regulatory element. J. Virol. 72, 5085–5092.

Drosten, C., Gunther, S., Preiser, W., van der Werf, S., Brodt, H.R., Becker, S., Rabenau, H., Panning, M., Kolesnikova, L., Fouchier, R.A., Berger, A., Burguiere, A.M., Cinatl, J., Eickmann, M., Escriou, N., Grywna, K., Kramme, S., Manuguerra, J.C., Muller, S., Rickerts, V., Sturmer, M., Vieth, S., Klenk, H.D., Osterhaus, A.D., Schmitz, H., Doerr, H.W., 2003. Identification of a novel coronavirus in patients with severe acute respiratory syndrome. N. Engl. J. Med. 348, 1967–1976.

Dupuis, M., Denis-Mize, K., Woo, C., Goldbeck, C., Selby, M.J., Chen, M., Otten, G.R., Ulmer, J.B., Donnelly, J.J., Ott, G., McDonald, D.M., 2000. Distribution of DNA vaccines determines their immunogenicity after intramuscular injection in mice. J. Immunol. 165, 2850–2858.

Ernst, R.K., Bray, M., Rekosh, D., Hammarskjold, M.L., 1997a. A structured retroviral RNA element that mediates nucleocytoplasmic export of intron-containing RNA. Mol. Cell. Biol. 17, 135–144.

Ernst, R.K., Bray, M., Rekosh, D., Hammarskjold, M.L., 1997b. Secondary structure and mutational analysis of the Mason-Pfizer monkey virus RNA constitutive transport element. RNA 3, 210–222.

Fouchier, R.A., Kuiken, T., Schutten, M., van Amerongen, G., van Doornum, G.J., van den Hoogen, B.G., Peiris, M., Lim, W., Stohr, K., Osterhaus, A.D., 2003. Aetiology: Koch's postulates fulfilled for SARS virus. Nature 423, 240.

Fu, T.M., Guan, L., Friedman, A., Schofield, T.L., Ulmer, J.B., Liu, M.A., Donnelly, J.J., 1999. Dose dependence of CTL precursor frequency induced by a DNA vaccine and correlation with protective immunity against influenza virus challenge. J. Immunol. 162, 4163–4170.

Fuerst, T.R., Niles, E.G., Studier, F.W., Moss, B., 1986. Eukaryotic transient-expression system based on recombinant vaccinia virus that synthesizes bacteriophage T7 RNA polymerase. Proc. Natl. Acad. Sci. U.S.A. 83, 8122–8126.

Garg, S., Oran, A.E., Hon, H., Jacob, J., 2004. The hybrid cytomegalovirus enhancer/chicken beta-actin promoter along with woodchuck hepatitis virus posttranscriptional regulatory element enhances the protective efficacy of DNA vaccines. J. Immunol. 173, 550–558.

Giroglou, T., Cinatl Jr., J., Rabenau, H., Drosten, C., Schwalbe, H., Doerr, H.W., von Laer, D., 2004. Retroviral vectors pseudotyped with severe acute respiratory syndrome coronavirus S protein. J. Virol. 78, 9007–9015.

Graf, M., Bojak, A., Deml, L., Bieler, K., Wolf, H., Wagner, R., 2000. Concerted action of multiple cis-acting sequences is required for Rev dependence of late human immunodeficiency virus type 1 gene expression. J. Virol. 74, 10822–10826.

Gruter, P., Tabernero, C., von Kobbe, C., Schmitt, C., Saavedra, C., Bachi, A., Wilm, M., Felber, B.K., Izaurralde, E., 1998. TAP, the human homolog of Mex67p, mediates CTE-dependent RNA export from the nucleus. Mol. Cell 1, 649–659.

Guan, Y., Zheng, B.J., He, Y.Q., Liu, X.L., Zhuang, Z.X., Cheung, C.L., Luo, S.W., Li, P.H., Zhang, L.J., Guan, Y.J., Butt, K.M., Wong, K.L., Chan, K.W., Lim, W., Shortridge, K.F., Yuen, K.Y., Peiris, J.S., Poon, L.L., 2003. Isolation and characterization of viruses related to the SARS coronavirus from animals in southern China. Science 302, 276–278.

Haijema, B.J., Volders, H., Rottier, P.J., 2003. Switching species tropism: an effective way to manipulate the feline coronavirus genome. J. Virol. 77, 4528–4538.

He, Y., Zhu, Q., Liu, S., Zhou, Y., Yang, B., Li, J., Jiang, S., 2005. Identification of a critical neutralization determinant of severe acute respiratory syndrome (SARS)-associated coronavirus: importance for designing SARS vaccines. Virology 334, 74–82.

Hofmann, H., Hattermann, K., Marzi, A., Gramberg, T., Geier, M., Krumbiegel, M., Kuate, S., Uberla, K., Niedrig, M., Pohlmann, S., 2004. S protein of severe acute respiratory syndrome-associated coronavirus mediates entry into hepatoma cell lines and is targeted by neutralizing antibodies in infected patients. J. Virol. 78, 6134–6142.

Horsburgh, B.C., Brown, T.D., 1995. Cloning, sequencing and expression of the S protein gene from two geographically distinct strains of canine coronavirus. Virus Res. 39, 63–74.

Huang, M.T., Gorman, C.M., 1990. Intervening sequences increase efficiency of RNA 3′ processing and accumulation of cytoplasmic RNA. Nucleic Acids Res. 18, 937–947.

Huang, Z.M., Yen, T.S., 1995. Role of the hepatitis B virus posttranscriptional regulatory element in export of intronless transcripts. Mol. Cell. Biol. 15, 3864–3869.

Huang, Y., Yang, Z.Y., Kong, W.P., Nabel, G.J., 2004. Generation of synthetic severe acute respiratory syndrome coronavirus pseudoparticles: implications for assembly and vaccine production. J. Virol. 78, 12557–12565.

Hull, S., Boris-Lawrie, K., 2003. Analysis of synergy between divergent simple retrovirus posttranscriptional control elements. Virology 317, 146–154.

Jeffers, S.A., Tusell, S.M., Gillim-Ross, L., Hemmila, E.M., Achenbach, J.E., Babcock, G.J., Thomas Jr., W.D., Thackray, L.B., Young, M.D., Mason, R.J., Ambrosino, D.M., Wentworth, D.E., Demartini, J.C., Holmes, K.V., 2004. CD209L (L-SIGN) is a receptor for severe acute respiratory syndrome coronavirus. Proc. Natl. Acad. Sci. U.S.A. 101, 15748–15753.

Jin, L., Guzik, B.W., Bor, Y.C., Rekosh, D., Hammarskjold, M.L., 2003. Tap and NXT promote translation of unspliced mRNA. Genes Dev. 17, 3075–3086.

Kan, B., Wang, M., Jing, H., Xu, H., Jiang, X., Yan, M., Liang, W., Zheng, H., Wan, K., Liu, Q., Cui, B., Xu, Y., Zhang, E., Wang, H., Ye, J., Li, G., Li, M., Cui, Z., Qi, X., Chen, K., Du, L., Gao, K., Zhao, Y.T., Zou, X.Z., Feng, Y.J., Gao, Y.F., Hai, R., Yu, D., Guan, Y., Xu, J., 2005. Molecular evolution analysis and geographic investigation of severe acute respiratory syndrome coronavirus-like virus in palm civets at an animal market and on farms. J. Virol. 79, 11892–11900.

Kang, Y., Cullen, B.R., 1999. The human Tap protein is a nuclear mRNA export factor that contains novel RNA-binding and nucleocytoplasmic transport sequences. Genes Dev. 13, 1126–1139.

Kotsopoulou, E., Kim, V.N., Kingsman, A.J., Kingsman, S.M., Mitrophanous, K.A., 2000. A Rev-independent human immunodeficiency virus type 1 (HIV-1)-based vector that exploits a codon-optimized HIV-1 gag-pol gene. J. Virol. 74, 4839–4852.

Krueger, D.K., Kelly, S.M., Lewicki, D.N., Ruffolo, R., Gallagher, T.M., 2001. Variations in disparate regions of the murine coronavirus spike protein impact the initiation of membrane fusion. J. Virol. 75, 2792–2802.

Ksiazek, T.G., Erdman, D., Goldsmith, C.S., Zaki, S.R., Peret, T., Emery, S., Tong, S., Urbani, C., Comer, J.A., Lim, W., Rollin, P.E., Dowell, S.F., Ling, A.E., Humphrey, C.D., Shieh, W.J., Guarner, J., Paddock, C.D., Rota, P., Fields, B., DeRisi, J., Yang, J.Y., Cox, N., Hughes, J.M., LeDuc, J.W., Bellini, W.J., Anderson, L.J., 2003. A novel coronavirus associated with severe acute respiratory syndrome. N. Engl. J. Med. 348, 1953–1966.

Kuo, L., Godeke, G.J., Raamsman, M.J., Masters, P.S., Rottier, P.J., 2000. Retargeting of coronavirus by substitution of the spike glycoprotein ectodomain: crossing the host cell species barrier. J. Virol. 74, 1393–1406.

Lau, S.K., Woo, P.C., Li, K.S., Huang, Y., Tsoi, H.W., Wong, B.H., Wong, S.S., Leung, S.Y., Chan, K.H., Yuen, K.Y., 2005. Severe acute respiratory syndrome coronavirus-like virus in Chinese horseshoe bats. Proc. Natl. Acad. Sci. U.S.A. 102, 14040–14045.

Lawler, J.V., Endy, T.P., Hensley, L.E., Garrison, A., Fritz, E.A., Lesar, M., Baric, R.S., Kulesh, D.A., Norwood, D.A., Wasieloski, L.P., Ulrich, M.P., Slezak, T.R., Vitalis, E., Huggins, J.W., Jahrling, P.B., Paragas, J., 2006. Cynomolgus macaque as an animal model for severe acute respiratory syndrome. PLoS Med. 3, e149.

Li, W., Moore, M.J., Vasilieva, N., Sui, J., Wong, S.K., Berne, M.A., Somasundaran, M., Sullivan, J.L., Luzuriaga, K., Greenough, T.C., Choe, H., Farzan, M., 2003. Angiotensin-converting enzyme 2 is a functional receptor for the SARS coronavirus. Nature 426, 450–454.

Li, W., Shi, Z., Yu, M., Ren, W., Smith, C., Epstein, J.H., Wang, H., Crameri, G., Hu, Z., Zhang, H., Zhang, J., McEachern, J., Field, H., Daszak, P., Eaton, B.T., Zhang, S., Wang, L.F., 2005. Bats are natural reservoirs of SARS-like coronaviruses. Science 310, 676–679.

Loeb, J.E., Cordier, W.S., Harris, M.E., Weitzman, M.D., Hope, T.J., 1999. Enhanced expression of transgenes from adeno-associated virus vectors with the woodchuck hepatitis virus posttranscriptional regulatory element: implications for gene therapy. Hum. Gene Ther. 10, 2295–2305.

Lu, S., Cullen, B.R., 2003. Analysis of the stimulatory effect of splicing on mRNA production and utilization in mammalian cells. RNA 9, 618–630.

Matsuyama, S., Ujike, M., Morikawa, S., Tashiro, M., Taguchi, F., 2005. Protease-mediated enhancement of severe acute respiratory syndrome coronavirus infection. Proc. Natl. Acad. Sci. U.S.A. 102, 12543–12547.

McAuliffe, J., Vogel, L., Roberts, A., Fahle, G., Fischer, S., Shieh, W.J., Butler, E., Zaki, S., St Claire, M., Murphy, B., Subbarao, K., 2004. Replication of SARS coronavirus administered into the respiratory tract of African Green, rhesus and cynomolgus monkeys. Virology 330, 8–15.

Nakamura, Y., October 2006, posting date. Homo sapiens codon usage table. [Online.] http://www.kazusa.or.jp/codon/cgi-bin/showcodon.cgi?species=Homo+sapiens=[gbpri].

Nakamura, Y., Gojobori, T., Ikemura, T., 2000. Codon usage tabulated from international DNA sequence databases: status for the year 2000. Nucleic Acids Res. 28, 292.

Nal, B., Chan, C., Kien, F., Siu, L., Tse, J., Chu, K., Kam, J., Staropoli, I., Crescenzo-Chaigne, B., Escriou, N., van der Werf, S., Yuen, K.Y., Altmeyer, R., 2005. Differential maturation and subcellular localization of severe acute respiratory syndrome coronavirus surface proteins S, M and E. J. Gen. Virol. 86, 1423–1434.

Narayanan, K., Chen, C.J., Maeda, J., Makino, S., 2003. Nucleocapsid-independent specific viral RNA packaging via viral envelope protein and viral RNA signal. J. Virol. 77, 2922–2927.

Nguyen, K.L., llano, M., Akari, H., Miyagi, E., Poeschla, E.M., Strebel, K., Bour, S., 2004. Codon optimization of the HIV-1 vpu and vif genes stabilizes their mRNA and allows for highly efficient Rev-independent expression. Virology 319, 163–175.

Nie, Y., Wang, G., Shi, X., Zhang, H., Qiu, Y., He, Z., Wang, W., Lian, G., Yin, X., Du, L., Ren, L., Wang, J., He, X., Li, T., Deng, H., Ding, M., 2004. Neutralizing antibodies in patients with severe acute respiratory syndrome-associated coronavirus infection. J. Infect. Dis. 190, 1119–1126.

Nott, A., Meislin, S.H., Moore, M.J., 2003. A quantitative analysis of intron effects on mammalian gene expression. RNA 9, 607–617.

Oberg, D., Collier, B., Zhao, X., Schwartz, S., 2003. Mutational inactivation of two distinct negative RNA elements in the human papillomavirus type 16 L2 coding region induces production of high levels of L2 in human cells. J. Virol. 77, 11674–11684.

Otten, G., Schaefer, M., Doe, B., Liu, H., Srivastava, I., zur Megede, J., O'Hagan, D., Donnelly, J., Widera, G., Rabussay, D., Lewis, M.G., Barnett, S., Ulmer, J.B., 2004. Enhancement of DNA vaccine potency in rhesus macaques by electroporation. Vaccine 22, 2489–2493.

Pertl, U., Wodrich, H., Ruehlmann, J.M., Gillies, S.D., Lode, H.N., Reisfeld, R.A., 2003. Immunotherapy with a posttranscriptionally modified DNA vaccine induces complete protection against metastatic neuroblastoma. Blood 101, 649–654.

Petit, C.M., Melancon, J.M., Chouljenko, V.N., Colgrove, R., Farzan, M., Knipe, D.M., Kousoulas, K.G., 2005. Genetic analysis of the SARS-coronavirus spike glycoprotein functional domains involved in cell-surface expression and cell-to-cell fusion. Virology 341, 215–230.

Petitclerc, D., Attal, J., Theron, M.C., Bearzotti, M., Bolifraud, P., Kann, G., Stinnakre, M.G., Pointu, H., Puissant, C., Houdebine, L.M., 1995. The effect of various introns and transcription terminators on the efficiency of expression vectors in various cultured cell lines and in the mammary gland of transgenic mice. J. Biotechnol. 40, 169–178.

Popa, I., Harris, M.E., Donello, J.E., Hope, T.J., 2002. CRM1-dependent function of a cis-acting RNA export element. Mol. Cell. Biol. 22, 2057–2067.

Promega, January 2004, revision date. pCI and pSI mammalian expression vectors. Technical bulletin. [Online.] http://www.promega.com/tbs/tb206/tb206.pdf.

Pulford, D.J., Britton, P., 1991. Intracellular processing of the porcine coronavirus transmissible gastroenteritis virus spike protein expressed by recombinant vaccinia virus. Virology 182, 765–773.

Qin, Z.L., Zhao, P., Zhang, X.L., Yu, J.G., Cao, M.M., Zhao, L.J., Luan, J., Qi, Z.T., 2004. Silencing of SARS-CoV spike gene by small interfering RNA in HEK 293T cells. Biochem. Biophys. Res. Commun. 324, 1186–1193.

Qu, X.X., Hao, P., Song, X.J., Jiang, S.M., Liu, Y.X., Wang, P.G., Rao, X., Song, H.D., Wang, S.Y., Zuo, Y., Zheng, A.H., Luo, M., Wang, H.L., Deng, F., Wang, H.Z., Hu, Z.H., Ding, M.X., Zhao, G.P., Deng, H.K., 2005. Identification of two critical amino acid residues of the severe acute respiratory syndrome coronavirus spike protein for its variation in zoonotic tropism transition via a double substitution strategy. J. Biol. Chem. 280, 29588–29595.

Reed, L.J., Muench, H., 1938. A simple method of estimating fifty percent endpoints. Am. J. Hyg. 27, 493–497.

Rizvi, T.A., Lew, K.A., Murphy Jr., E.C., Schmidt, R.D., 1996. Role of Mason-Pfizer monkey virus (MPMV) constitutive transport element (CTE) in the propagation of MPMV vectors by genetic complementation using homologous/heterologous env genes. Virology 224, 517–532.

Rota, P.A., Oberste, M.S., Monroe, S.S., Nix, W.A., Campagnoli, R., Icenogle, J.P., Penaranda, S., Bankamp, B., Maher, K., Chen, M.H., Tong, S., Tamin, A., Lowe, L., Frace, M., DeRisi, J.L., Chen, Q., Wang, D., Erdman, D.D., Peret, T.C., Burns, C., Ksiazek, T.G., Rollin, P.E., Sanchez, A., Liffick, S., Holloway, B., Limor, J., McCaustland, K., Olsen-Rasmussen, M., Fouchier, R., Gunther, S., Osterhaus, A.D., Drosten, C., Pallansch, M.A., Anderson, L.J., Bellini, W.J., 2003. Characterization of a novel coronavirus associated with severe acute respiratory syndrome. Science 300, 1394–1399.

Rowe, T., Gao, G., Hogan, R.J., Crystal, R.G., Voss, T.G., Grant, R.L., Bell, P., Kobinger, G.P., Wivel, N.A., Wilson, J.M., 2004. Macaque model for severe acute respiratory syndrome. J. Virol. 78, 11401–11404.

Schambach, A., Wodrich, H., Hildinger, M., Bohne, J., Krausslich, H.G., Baum, C., 2000. Context dependence of different modules for posttranscriptional enhancement of gene expression from retroviral vectors. Mol. Ther. 2, 435–445.

Schwegmann-Wessels, C., Al-Falah, M., Escors, D., Wang, Z., Zimmer, G., Deng, H., Enjuanes, L., Naim, H.Y., Herrler, G., 2004. A novel sorting signal for intracellular localization is present in the S protein of a porcine coronavirus but absent from severe acute respiratory syndrome-associated coronavirus. J. Biol. Chem. 279, 43661–43666.

Simmons, G., Reeves, J.D., Rennekamp, A.J., Amberg, S.M., Piefer, A.J., Bates, P., 2004. Characterization of severe acute respiratory syndrome-associated coronavirus (SARS-CoV) spike glycoprotein-mediated viral entry. Proc. Natl. Acad. Sci. U.S.A. 101, 4240–4245.

Simmons, G., Gosalia, D.N., Rennekamp, A.J., Reeves, J.D., Diamond, S.L., Bates, P., 2005. Inhibitors of cathepsin L prevent severe acute respiratory syndrome coronavirus entry. Proc. Natl. Acad. Sci. U.S.A. 102, 11876–11881.

Song, H.D., Tu, C.C., Zhang, G.W., Wang, S.Y., Zheng, K., Lei, L.C., Chen, Q.X., Gao, Y.W., Zhou, H.Q., Xiang, H., Zheng, H.J., Chern, S.W., Cheng, F., Pan, C.M., Xuan, H., Chen, S.J., Luo, H.M., Zhou, D.H., Liu, Y.F., He, J.F., Qin, P.Z., Li, L.H., Ren, Y.Q., Liang, W.J., Yu, Y.D., Anderson, L., Wang, M., Xu, R.H., Wu, X.W., Zheng, H.Y., Chen, J.D., Liang, G., Gao, Y., Liao, M., Fang, L., Jiang, L.Y., Li, H., Chen, F., Di, B., He, L.J., Lin, J.Y., Tong, S., Kong, X., Du, L., Hao, P., Tang, H., Bernini, A., Yu, X.J., Spiga, O., Guo, Z.M., Pan, H.Y., He, W.Z., Manuguerra, J.C., Fontanet, A., Danchin, A., Niccolai, N., Li, Y.X., Wu, C.I., Zhao, G.P., 2005. Cross-host evolution of severe acute respiratory syndrome coronavirus in palm civet and human. Proc. Natl. Acad. Sci. U.S.A. 102, 2430–2435.

Subbarao, K., McAuliffe, J., Vogel, L., Fahle, G., Fischer, S., Tatti, K., Packard, M., Shieh, W.J., Zaki, S., Murphy, B., 2004. Prior infection and passive transfer of neutralizing antibody prevent replication of severe acute respiratory syndrome coronavirus in the respiratory tract of mice. J. Virol. 78, 3572–3577.

Tan, W., Felber, B.K., Zolotukhin, A.S., Pavlakis, G.N., Schwartz, S., 1995. Efficient expression of the human papillomavirus type 16 L1 protein in epithelial cells by using Rev and the Rev-responsive element of human immunodeficiency virus or the cis-acting transactivation element of simian retrovirus type 1. J. Virol. 69, 5607–5620.

Temperton, N.J., 2005. Longitudinally profiling neutralizing antibody response to SARS coronavirus with pseudotypes. Emerg. Infect. Dis. 11, 411–416.

ter Meulen, J., Bakker, A.B., van den Brink, E.N., Weverling, G.J., Martina, B.E., Haagmans, B.L., Kuiken, T., de Kruif, J., Preiser, W., Spaan, W., Gelderblom, H.R., Goudsmit, J., Osterhaus, A.D., 2004. Human monoclonal antibody as prophylaxis for SARS coronavirus infection in ferrets. Lancet 363, 2139–2141.

The Chinese SARS Molecular Epidemiology Consortium, 2004. Molecular evolution of the SARS coronavirus during the course of the SARS epidemic in China. Science 303, 1666–1669.

Traggiai, E., Becker, S., Subbarao, K., Kolesnikova, L., Uematsu, Y., Gismondo, M.R., Murphy, B.R., Rappuoli, R., Lanzavecchia, A., 2004. An efficient method to make human monoclonal antibodies from memory B cells: potent neutralization of SARS coronavirus. Nat. Med. 10, 871–875.

Tu, C., Crameri, G., Kong, X., Chen, J., Sun, Y., Yu, M., Xiang, H., Xia, X., Liu, S., Ren, T., Yu, Y., Eaton, B.T., Xuan, H., Wang, L.F., 2004. Antibodies to SARS coronavirus in civets. Emerg. Infect. Dis. 10, 2244–2248.

Ulmer, J.B., Deck, R.R., DeWitt, C.M., Friedman, A., Donnelly, J.J., Liu, M.A., 1994. Protective immunity by intramuscular injection of low doses of influenza virus DNA vaccines. Vaccine 12, 1541–1544.

Vennema, H., Godeke, G.J., Rossen, J.W., Voorhout, W.F., Horzinek, M.C., Opstelten, D.J., Rottier, P.J., 1996. Nucleocapsid-independent assembly of coronavirus-like particles by co-expression of viral envelope protein genes. EMBO J. 15, 2020–2028.

Wang, S., Liu, X., Fisher, K., Smith, J.G., Chen, F., Tobery, T.W., Ulmer, J.B., Evans, R.K., Caulfield, M.J., 2000. Enhanced type I immune response to a hepatitis B DNA vaccine by formulation with calcium- or aluminum phosphate. Vaccine 18, 1227–1235.

Wang, L., Menon, S., Bolin, S.R., Bello, L.J., 2003. A hepadnavirus regulatory element enhances expression of a type 2 bovine viral diarrhea virus E2 protein from a bovine herpesvirus 1 vector. J. Virol. 77, 8775–8782.

Wang, S., Chou, T.H., Sakhatskyy, P.V., Huang, S., Lawrence, J.M., Cao, H., Huang, X., Lu, S., 2005a. Identification of two neutralizing regions on the severe acute respiratory syndrome coronavirus spike glycoprotein produced from the mammalian expression system. J. Virol. 79, 1906–1910.

Wang, Z., Yuan, Z., Matsumoto, M., Hengge, U.R., Chang, Y.F., 2005b. Immune responses with DNA vaccines encoded different gene fragments of severe acute respiratory syndrome coronavirus in BALB/c mice. Biochem. Biophys. Res. Commun. 327, 130–135.

WHO, 21 April 2004, posting date. Summary of probable SARS cases with onset of illness from 1 November 2002 to 31 July 2003. [Online.] http://www.who.int/csr/sars/country/table2004_04_21/en/index.html.

WHO, October 2004, posting date. WHO guidelines for the global surveillance of severe acute respiratory syndrome (SARS). [Online.] http://www.who.int/csr/resources/publications/WHO_CDS_CSR_ARO_2004_1/en/index.html.

Wodrich, H., Schambach, A., Krausslich, H.G., 2000. Multiple copies of the Mason-Pfizer monkey virus constitutive RNA transport element lead to enhanced HIV-1 Gag expression in a context-dependent manner. Nucleic Acids Res. 28, 901–910.

Wu, D., Tu, C., Xin, C., Xuan, H., Meng, Q., Liu, Y., Yu, Y., Guan, Y., Jiang, Y., Yin, X., Crameri, G., Wang, M., Li, C., Liu, S., Liao, M., Feng, L., Xiang, H., Sun, J., Chen, J., Sun, Y., Gu, S., Liu, N., Fu, D., Eaton, B.T., Wang, L.F., Kong, X., 2005. Civets are equally susceptible to experimental infection by two different severe acute respiratory syndrome coronavirus isolates. J. Virol. 79, 2620–2625.

Xiao, X., Chakraborti, S., Dimitrov, A.S., Gramatikoff, K., Dimitrov, D.S., 2003. The SARS-CoV S glycoprotein: expression and functional characterization. Biochem. Biophys. Res. Commun. 312, 1159–1164.

Yang, Z.Y., Kong, W.P., Huang, Y., Roberts, A., Murphy, B.R., Subbarao, K., Nabel, G.J., 2004. A DNA vaccine induces SARS coronavirus neutralization and protective immunity in mice. Nature 428, 561–564.

Yang, Z.Y., Werner, H.C., Kong, W.P., Leung, K., Traggiai, E., Lanzavecchia, A., Nabel, G.J., 2005. Evasion of antibody neutralization in emerging severe acute respiratory syndrome coronaviruses. Proc. Natl. Acad. Sci. U.S.A. 102, 797–801.

Yi, C.E., Ba, L., Zhang, L., Ho, D.D., Chen, Z., 2005. Single amino acid substitutions in the severe acute respiratory syndrome coronavirus spike glycoprotein determine viral entry and immunogenicity of a major neutralizing domain. J. Virol. 79, 11638–11646.

Yoo, D., Deregt, D., 2001. A single amino acid change within antigenic domain II of the spike protein of bovine coronavirus confers resistance to virus neutralization. Clin. Diagn. Lab. Immunol. 8, 297–302.

Zennou, V., Petit, C., Guetard, D., Nerhbass, U., Montagnier, L., Charneau, P., 2000. HIV-1 genome nuclear import is mediated by a central DNA flap. Cell 101, 173–185.

Zhi, Y., Kobinger, G.P., Jordan, H., Suchma, K., Weiss, S.R., Shen, H., Schumer, G., Gao, G., Boyer, J.L., Crystal, R.G., Wilson, J.M., 2005. Identification of murine CD8 T cell epitopes in codon-optimized SARS-associated coronavirus spike protein. Virology 335, 34–45.

Zufferey, R., Donello, J.E., Trono, D., Hope, T.J., 1999. Woodchuck hepatitis virus posttranscriptional regulatory element enhances expression of transgenes delivered by retroviral vectors. J. Virol. 73, 2886–2892.